

See discussions, stats, and author profiles for this publication at: <https://www.researchgate.net/publication/319023776>

# Constraining the subsoil carbon source to cave-air CO<sub>2</sub> and speleothem calcite in central Texas

Article in *Geochimica et Cosmochimica Acta* · August 2017

DOI: 10.1016/j.gca.2017.08.017

---

CITATIONS

2

---

READS

129

7 authors, including:



[Shelly Bergel](#)

Hebrew University of Jerusalem

3 PUBLICATIONS 12 CITATIONS

[SEE PROFILE](#)



[Jay L Banner](#)

University of Texas at Austin

186 PUBLICATIONS 5,512 CITATIONS

[SEE PROFILE](#)



# Constraining the subsoil carbon source to cave-air CO<sub>2</sub> and speleothem calcite in central Texas

Shelly J. Bergel<sup>a,\*</sup>, Peter E. Carlson<sup>a</sup>, Toti E. Larson<sup>a</sup>, Chris T. Wood<sup>b</sup>,  
Kathleen R. Johnson<sup>b</sup>, Jay L. Banner<sup>a</sup>, Daniel O. Breecker<sup>a</sup>

<sup>a</sup> The Department of Geological Sciences, The University of Texas at Austin, 1 University Station, C1100, Austin, TX 78712-0254, USA

<sup>b</sup> Department of Earth System Science, University of California, 3200 Croul Hall, Irvine, CA 92697-3100, USA

Received 17 December 2016; accepted in revised form 5 August 2017; Available online 9 August 2017

## Abstract

Canonical models for speleothem formation and the subsurface carbon cycle invoke soil respiration as the dominant carbon source. However, evidence from some karst regions suggests that belowground CO<sub>2</sub> originates from a deeper, older source. We therefore investigated the carbon sources to central Texas caves. Drip-water chemistry of two caves in central Texas implies equilibration with calcite at CO<sub>2</sub> concentrations ( $P_{\text{CO}_2\text{-sat}}$ ) higher than the maximum CO<sub>2</sub> concentrations observed in overlying soils. This observation suggests that CO<sub>2</sub> is added to waters after they percolate through the soils, which requires a subsoil carbon source. We directly evaluate the carbon isotope composition of the subsoil carbon source using  $\delta^{13}\text{C}$  measurements on cave-air CO<sub>2</sub>, which we independently demonstrate has little to no contribution from host rock carbon. We do so using the oxidative ratio, OR, defined as the number of moles of O<sub>2</sub> consumed per mole of CO<sub>2</sub> produced during respiration. However, additional belowground processes that affect O<sub>2</sub> and CO<sub>2</sub> concentrations, such as gas-water exchange and/or diffusion, may also influence the measured oxidative ratio, yielding an apparent OR ( $\text{OR}_{\text{apparent}}$ ). Cave air in Natural Bridge South Cavern has  $\text{OR}_{\text{apparent}}$  values ( $1.09 \pm 0.06$ ) indistinguishable from those expected for respiration alone ( $1.08 \pm 0.06$ ). Pore space gases from soils above the cave have lower values ( $\text{OR}_{\text{apparent}} = 0.67 \pm 0.05$ ) consistent with respiration and gas transport by diffusion. The simplest explanation for these observations is that cave air in NB South is influenced by respiration in open-system bedrock fractures such that neither diffusion nor exchange with water influence the composition of the cave air. The radiocarbon activities of NB South cave-air CO<sub>2</sub> suggest the subsoil carbon source is hundreds of years old. The calculated  $\delta^{13}\text{C}$  values of the subsoil carbon source are consistent with tree-sourced carbon (perhaps decomposing root matter), the  $\delta^{13}\text{C}$  values of which have shifted during industrialization due to changes in the  $\delta^{13}\text{C}$  values and concentrations of atmospheric CO<sub>2</sub>. Seasonal variations in  $P_{\text{CO}_2\text{-sat}}$  in most of the drip waters suggest that these waters exchange with ventilated bedrock fractures in the epikarst, implying that the subsoil CO<sub>2</sub> source contributes carbon to speleothems.

© 2017 Elsevier Ltd. All rights reserved.

**Keywords:** Oxidative ratio; Carbon isotopes; Respired CO<sub>2</sub>; Cave air; Drip water

\* Corresponding author at: The Fredy and Nadine Herrmann Institute of Earth Sciences, Hebrew University of Jerusalem, Jerusalem 91904, Israel.

E-mail addresses: [shelly.bergel@mail.huji.ac.il](mailto:shelly.bergel@mail.huji.ac.il) (S.J. Bergel), [petercarlson@utexas.edu](mailto:petercarlson@utexas.edu) (P.E. Carlson), [totilarson@jsg.utexas.edu](mailto:totilarson@jsg.utexas.edu) (T.E. Larson), [ctwood@uci.edu](mailto:ctwood@uci.edu) (C.T. Wood), [kathleen.johnson@uci.edu](mailto:kathleen.johnson@uci.edu) (K.R. Johnson), [banner@jsg.utexas.edu](mailto:banner@jsg.utexas.edu) (J.L. Banner), [breecker@jsg.utexas.edu](mailto:breecker@jsg.utexas.edu) (D.O. Breecker).

<http://dx.doi.org/10.1016/j.gca.2017.08.017>

0016-7037/© 2017 Elsevier Ltd. All rights reserved.

## 1. INTRODUCTION

The subsoil region of the vadose zone is insufficiently studied compared to the overlying soil and underlying phreatic zones. Processes occurring in this intermediate zone are, however, especially important in karst regions, where this zone can be quite dynamic due to the presence

of substantial secondary porosity including caves and interconnected fracture networks. Of particular relevance to this study, the carbon cycle in this intermediate zone is poorly understood (Serrano-Ortiz et al., 2010). The canonical carbon cycling model invoking soil respiration as the dominant CO<sub>2</sub> source throughout the vadose zone (e.g., Hendy, 1971) is widely adopted despite substantial evidence from some karst regions for the importance of subsoil carbon sources to underground air (Atkinson, 1977; Wood and Petraitis, 1984; Wood et al., 1993; Noronha et al., 2015; Matthey et al., 2016; McDonough et al., 2016). This model assumes soil respiration as the CO<sub>2</sub> source for carbonic acid, which dissolves limestone, releasing Ca<sup>2+</sup> ions into solution that eventually precipitate as speleothems (Hendy, 1971). The soil CO<sub>2</sub> carbon source in this conceptual model influences the interpretation of variations in speleothem growth rates, chemical compositions, and δ<sup>13</sup>C values. Furthermore, accurate accounting of the global carbon cycle must include an understanding of carbon flows in karst (Serrano-Ortiz et al., 2010; White, 2013), which constitutes 13% of the global land surface (Amiotte Suchet et al., 2003). In this study, we report evidence that biological respiration in bedrock fractures rather than in the soil is the primary carbon source for caves and speleothems in central Texas. We also evaluate the carbon isotope composition of the subsoil carbon source in one cave that provides a unique opportunity to avoid the contribution of carbon from host rock limestone. Our findings are relevant for understanding subsurface carbon cycling and interpreting carbon isotope compositions of speleothem calcite for paleoclimate reconstructions.

## 2. BACKGROUND

In this study, we use the oxidative ratio (OR), which is the ratio of moles of O<sub>2</sub> consumed to moles of CO<sub>2</sub> produced during respiration. We define the OR value relative to atmospheric air, and calculate OR using O<sub>2</sub> and CO<sub>2</sub> measurements in soil gas and cave air.

$$\text{OR}_{\text{apparent}} = -\left(\frac{\Delta\text{O}_2/\text{Ar}}{\Delta\text{CO}_2/\text{Ar}}\right) \quad (1)$$

where Δ refers to the sample (soil gas or cave air) deviation from the average atmospheric composition ( $\Delta\text{O}_2/\text{Ar} = [\text{O}_2/\text{Ar}]_{\text{sample}} - [\text{O}_2/\text{Ar}]_{\text{atm air}}$  and  $\Delta\text{CO}_2/\text{Ar} = [\text{CO}_2/\text{Ar}]_{\text{sample}} - [\text{CO}_2/\text{Ar}]_{\text{atm air}}$ ). Ratios to Ar improve precision as described below. We also use stable carbon isotope ratios of CO<sub>2</sub> to help constrain carbon sources. This section describes the effect of various processes on apparent values of OR (OR<sub>apparent</sub>) and the stable carbon isotope ratios of CO<sub>2</sub> in soil gas and underground air.

### 2.1. The oxidative ratio and controls on subsurface CO<sub>2</sub> and O<sub>2</sub> concentrations

Aerobic respiration produces CO<sub>2</sub> and consumes O<sub>2</sub>. This process, as well as any other process that affects CO<sub>2</sub> and O<sub>2</sub> concentrations, can be detected by measuring the apparent oxidative ratio (OR<sub>apparent</sub>), which in soils has a value of close to but not exactly 1.0 (Dilly, 2001; Hockaday et al., 2009; Clay and Worrall, 2015a,b). Diffu-

sion also influences belowground CO<sub>2</sub> and O<sub>2</sub> concentrations whereas advection does not. As net diffusion is dictated by a concentration gradient, CO<sub>2</sub> and O<sub>2</sub> molecules undergo a net flux from the soil to atmosphere and from the atmosphere to soil, respectively. More rapid diffusion of O<sub>2</sub> than CO<sub>2</sub> due to a difference in molecular mass (Massman, 1998) results in less O<sub>2</sub> depletion in soil than expected given the CO<sub>2</sub> concentration measured in a gas mixture. In other words, diffusion results in lower apparent than actual OR. This effect of diffusion is predictable and relatively constant leading to a diffusion signature, which we use in this study to help trace whether cave-air CO<sub>2</sub> originated from the soil, where gas transport is dominated by diffusion, or from the subsoil vadose zone, where gas transport is dominated by advection (Covington, 2015).

Exchange of CO<sub>2</sub> and O<sub>2</sub> between gas and water in a closed system also has effects on belowground CO<sub>2</sub> and O<sub>2</sub> concentrations that are distinct from respiration. Due to the relatively low solubility of O<sub>2</sub> in water, gas-water exchange has a negligible effect on O<sub>2</sub> concentrations unless the water/gas volume ratio is very high. For instance, limestone dissolution in a closed system will consume CO<sub>2</sub> without changing O<sub>2</sub>. In addition, water in equilibrium with gas in the soil or subsoil vadose zone that subsequently flows into a cave will degas CO<sub>2</sub> while consuming a negligible amount of O<sub>2</sub>. Therefore, in addition to being a tracer for transport by diffusion, CO<sub>2</sub> and O<sub>2</sub> concentrations in cave air can also help identify the extent to which a vadose zone system is opened or closed and help determine whether CO<sub>2</sub> is transported into caves as a gas or dissolved in seepage waters.

### 2.2. Soil CO<sub>2</sub>, soil-respired CO<sub>2</sub> and their stable carbon isotope ratios

The δ<sup>13</sup>C values of soil pore space CO<sub>2</sub> (soil CO<sub>2</sub>) are controlled by 1) the δ<sup>13</sup>C values of CO<sub>2</sub> respired in the soil (soil-respired CO<sub>2</sub>, δ<sup>13</sup>C<sub>r</sub>), 2) mixing with atmospheric CO<sub>2</sub> and 3) escape from belowground into the atmosphere by diffusion. Microbial and plant root respiration in soils produce CO<sub>2</sub> with δ<sup>13</sup>C values that are lower than that of atmospheric CO<sub>2</sub> and, therefore, high rates of respiration will decrease the δ<sup>13</sup>C values of soil CO<sub>2</sub> by increasing the mixing ratio of soil-respired CO<sub>2</sub> (Cerling et al., 1991). Accumulation of respired CO<sub>2</sub> in soil pore spaces results in net diffusion of CO<sub>2</sub> into the atmosphere. Preferential escape of <sup>12</sup>CO<sub>2</sub> compared with <sup>13</sup>CO<sub>2</sub> during diffusion increases the δ<sup>13</sup>C value of the residual soil pore space CO<sub>2</sub> by +4.4‰ at steady state (Cerling et al., 1991). Thus, calculating soil δ<sup>13</sup>C<sub>r</sub> values requires two steps 1) using a Keeling plot approach (δ<sup>13</sup>C vs. 1/CO<sub>2</sub>) to mathematically isolate and remove the atmospheric component and 2) subtracting 4.4‰ from the Keeling plot y-intercept to account for diffusion. At high respiration rates (or low porosity or any other factor that elevates belowground CO<sub>2</sub> concentration), the atmospheric component is relatively small and soil CO<sub>2</sub> δ<sup>13</sup>C values can reach a minimum of 4.4‰ higher than δ<sup>13</sup>C<sub>r</sub> values. At low respiration rates, the atmospheric component can be substantial and soil CO<sub>2</sub> δ<sup>13</sup>C values are more than 4.4‰ higher than δ<sup>13</sup>C<sub>r</sub> values. This theory is

widely applied to soils and forms the basis for interpreting  $\delta^{13}\text{C}$  values of soil carbonates, including the paleosol carbonate atmospheric  $\text{CO}_2$  proxy (Cerling, 1991).

Whether or not the +4.4‰ diffusion correction applies to deeper, subsoil underground air and specifically whether it applies to the  $\text{CO}_2$  source for speleothems is poorly understood. The canonical model for speleothem formation in which the  $\text{CO}_2$  originates in the soil suggests that it should apply to caves and speleothems; this would mean that the 4.4‰ correction would need to be applied if  $\delta^{13}\text{C}$  values of the organic carbon source were to be calculated from speleothem  $\delta^{13}\text{C}$  values. To investigate this, Breecker et al. (2012) compared  $\delta^{13}\text{C}$  values of respired  $\text{CO}_2$  calculated from measurements of cave-air  $\text{CO}_2$  and soil  $\text{CO}_2$ . The agreement between  $\delta^{13}\text{C}_r$  values of soil gas under trees and cave-air values was interpreted as a tree carbon source to cave-air  $\text{CO}_2$ . Measurements of  $\delta^{13}\text{C}$  values of drip water dissolved inorganic carbon (DIC) in the same caves were consistent with this interpretation, suggesting that speleothem calcite has the same carbon source as cave-air  $\text{CO}_2$  (Meyer et al., 2014). Implicit in this interpretation is that diffusion affects  $\delta^{13}\text{C}$  values of either soil and cave-air  $\text{CO}_2$  or that diffusion affects neither of them. In this paper, we use  $\text{OR}_{\text{apparent}}$  to help assess net transfer of below-ground  $\text{CO}_2$  by diffusion.

### 3. METHODS

#### 3.1. Study area

The two sample localities in this study are Natural Bridge Caverns (NB) and Inner Space Cavern (IS), both located on the Edwards Plateau in central Texas (Fig. 1). NB is located on the northern edge of San Antonio, and IS is 40 km north of central Austin, with 148 km separating the two caves. Both localities experience a similar subhumid to semiarid subtropical climate, with an average surface temperature of 29 °C in the summer and 12 °C in the winter. The area experiences an average precipitation of 870 mm (1981–2010; NOAA climate normals), with peak rainfall occurring during the late spring and, depending on the hurricane and tropical storm patterns, sometimes during the fall.

The Edwards Plateau is composed of karstified marine carbonates that formed during the early Cretaceous period, and contains caves with active speleothem deposition. NB is developed in the upper Glen Rose and lower Walnut Creek formations within interbedded limestone and dolomitic units. What used to be a single cavern at NB has been divided by collapse into two caverns, NB North (NBN) and NB South (NBS). IS is developed in the Edwards limestone, containing minor interbedded dolomite. NB has a transect length of 2621 m and a maximum depth of 76 m, while IS has a total passage length of 4851 m and a maximum depth of 24 m (Elliot and Veni, 1994). Cave volumes of NBN and NBS are 250,000 m<sup>3</sup> and 150,000 m<sup>3</sup>, respectively, and 75,000 m<sup>3</sup> at IS (Cowan et al., 2013). Both NB and IS are tourist caves, receiving the greatest number of visitors in mid-March and the months of May through August (Cowan et al., 2013). Ventilation fans have been

installed in both caves in order to prevent  $\text{CO}_2$  concentrations from becoming too high and causing visitor discomfort. During the study period, the ventilation fan at Inner Space Cavern was not operated, whereas the fan in Natural Bridge North (location of site NBCT) was operated once or twice a week between 12:00 and 16:00 from the end of June to the beginning of August (2% of the total time during JJAS), and the fan in Natural Bridge South Cavern (remainder of the NB sampling sites) operated continuously. It is possible that the operation of these ventilation fans causes our data to misrepresent the extent to which the natural epikarst network is an open or closed system (see Section 5.1). Regardless, it does not affect our conclusions about carbon sources. An excavated entrance tunnel at IS remains unsealed and in contact with the atmosphere. At both NB caves, the entrances are sealed by glass doors that remain shut except when tour groups enter and exit. The surrounding area of IS has undergone extensive and intermittent construction and development over the past ~50 years. NB is in a less urbanized area than IS, but construction has increased over the past several years to develop tourist attractions. There has been 8000 m<sup>2</sup> of brush clearing above NB that has had an observable effect on  $\text{CO}_2$  concentration in cave-air and speleothem deposition (Wong and Banner, 2010).

Above both caves, soils range in thickness from 0 to 35 cm and contain fragments of the underlying bedrock. These soils are clay-rich Mollisols that support oak and juniper savannah and patches of woodland and grassland (Cooke et al., 2007; Breecker et al., 2012). Soils above NB consist of extremely stony clays and gravely clay loams. Soils above IS consist of silty clays and stony clays (U.S. Department of Agriculture, Web Soil Survey).

The most prevalent tree species above both caves are *Juniperus ashei* (Ashe juniper) and *Quercus virginiana* (Texas live oak). Grasslands consist of the C<sub>4</sub> species *Bothriochloa ischaemum* (king ranch bluestem) and *Carex planostachys* (cedar Sedge), and few C<sub>3</sub> plants. *Opuntia engelmannii* (Texas prickly pear cactus), a CAM plant, grows in patches in less forested areas. Jackson et al. (1999) studied the rooting depth reached by woody plants in caves on the Edwards Plateau. The results indicate that the maximum rooting depth into bedrock of the ecosystem is 25 m. Specifically, the maximum observed rooting depth of *Juniperus ashei* is 8 m and of *Quercus virginiana* var. *fusiformis* is ~20 m.

#### 3.2. Field methods

Drip waters were collected for measurement of pH, alkalinity,  $\delta^{13}\text{C}$  values of DIC, and <sup>14</sup>C activity of DIC. For collection of water samples for  $\delta^{13}\text{C}$  DIC measurement, 0.4 mL of sample water was injected into round-bottomed septum-capped, UHP He-flushed Labco Exetainer<sup>®</sup> vials depressurized to atmospheric pressure before sample injection. For collection of water samples for DIC <sup>14</sup>C activity measurements, 30–100 mL of drip water were directly collected in 100 mL Corning Pyrex<sup>®</sup> storage bottles with polypropylene plug seal caps. Given the cave-air pCO<sub>2</sub> and temperature, the headspace contributes no more than

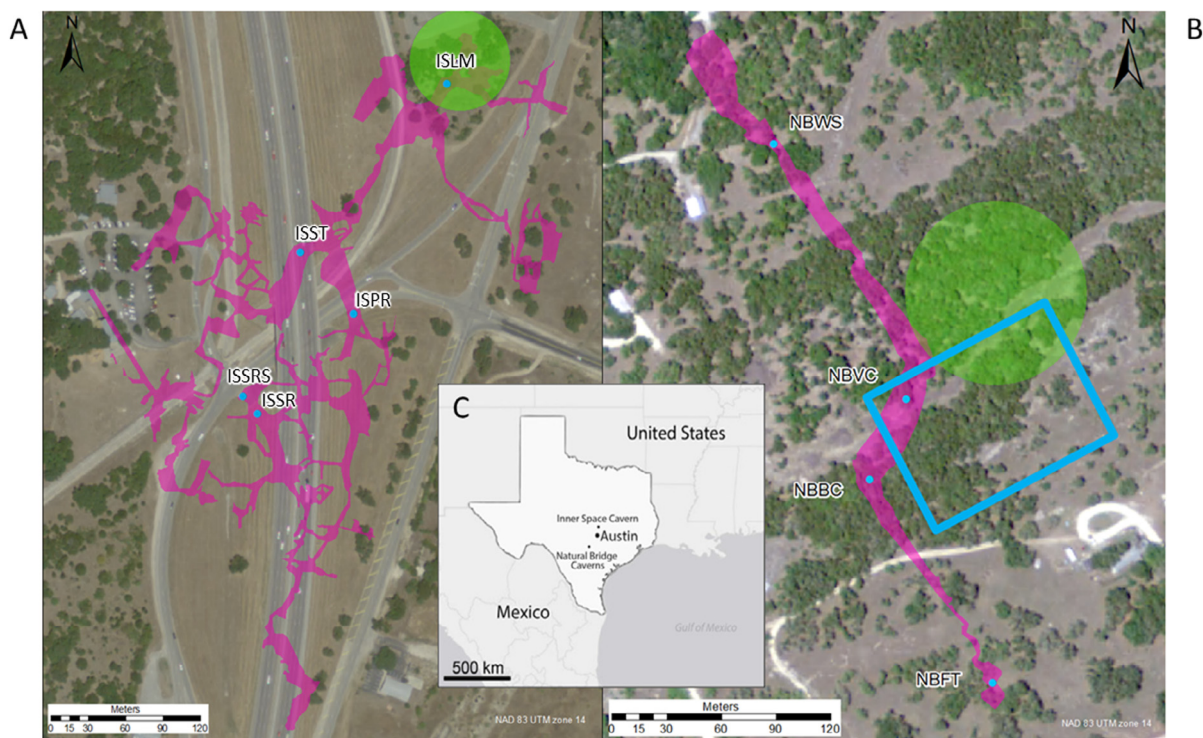


Fig. 1. Cave map outlines of Inner Space (A) and Natural Bridge South (B) Caverns, showing cave air sampling locations as blue dots and soil-gas sampling areas within the green circles. The blue rectangle in (B) represents the area of vegetative clearing in Wong and Banner (2010). NBCT is a sampling location not shown on this map, as it is in Natural Bridge North and was not a regular sample collection site. Cave site locations are shown in (C), which was adapted from Meyer et al. (2014). (For interpretation of the references to colour in this figure legend, the reader is referred to the web version of this article.)

6% (worst-case scenario of 30 mL of water and 70 mL of cave air in each bottle) of the total carbon to the sample bottle system. Therefore, considering the measured radio-carbon activity of cave air, adjustments to account for contamination of water samples by C in cave air are only slightly larger than the analytical error of the  $^{14}\text{C}$  measurements themselves. Before collection, these bottles were rinsed with 10% HCl and baked at 300 °C under vacuum for 2 h.

Cave-air and soil-gas samples were collected from IS and NB on a monthly basis from May to October 2014, when cave-air  $\text{CO}_2$  concentrations were substantially elevated above atmospheric values, to allow determination of  $\text{OR}_{\text{apparent}}$ . Samples were collected by first evacuating a septum-capped glass vial (Labco exetainer<sup>®</sup>) in the field and then flushing the vial with soil or cave air several times. This was achieved using a 12 V battery-powered vacuum pump (KNF Neuberger Inc., part #UN84.4ANDC-B). The inlet of the vacuum pump was connected to the septum-capped vial using plastic tubing with a 1/4" outer diameter and 1/8" inner diameter. A needle at the end of the tubing penetrated the septum on the vial. Another length of the same type of tubing connected the vial to the gas samples (via a soil-gas well for soil-gas samples, described below). Five replicates of atmospheric air were collected during each cave trip. Cave-air samples were collected along a transect, from the outer-most regions closest

to atmospheric exposure to greater depths inward. Cave air was collected from a total of five locations at NB (WS, BC, VC, FT, and CT) and IS (SR, SRS, ST, LM, and PR), with a sample and a replicate collected at each location (Fig. 1). Soil gas was collected from septum-capped stainless steel gas wells that were installed at multiple locations above the caverns. These wells were crimped at the bottom, and contained ~2 mm wide slits in the side wall just above the crimp. They were inserted into the soil vertically using a battery-powered drill, and were subsequently capped with a 1/4" Swagelok<sup>®</sup> union and a 1/4"–1/8" reducing port connector, fitted with a rubber septum to make a seal. Design of these wells is described more in detail in Breecker and Sharp (2008); the only difference in this study is that the wells were installed vertically and 1/16" tubing was not used. At most soil collection sites, two wells were installed: one reaching 15 cm deep (shallow) and the other reaching 30 cm deep (deep). When soil thickness was less than 30 cm, only the shallow well was installed. At IS, soil-gas samples were collected from wells beneath three Ashe junipers, three Texas live oaks, and three cedar elms, for a total of seventeen wells (two wells beneath each tree, besides one juniper, in which only a shallow well was installed). At NB, soil-gas wells were installed beneath three Ashe junipers, three Texas live oaks, one cedar elm, and at three grassland patches. Two wells were installed under oak, elm and two of the junipers and one well was installed at the grass sites

and the third juniper for a total of sixteen wells (Fig. 1); however, one grass well and one juniper well were lost midway through the collection period.

Gas samples for radiocarbon analysis of CO<sub>2</sub> were collected during winter 2013, spring 2013, and summer 2015. Samples were collected using 1 L (soil gas) and 2 L (cave air) evacuated glass flasks fitted with Teflon stopcocks. Before sample collection, these flasks were washed with 10% HCl and heated under vacuum to 400–500 °C for 15 min using an oxygen flame torch. These sample flasks were shipped within a month of sample collection to the University of California, Irvine for measurement of <sup>14</sup>C activity.

### 3.3. Analytical methods

Drip-water pH was measured in the field using a Myron L. Ultrameter II. Alkalinity was measured by single-endpoint manual titration to pH 4.50 ± 0.02 using 0.1 N H<sub>2</sub>SO<sub>4</sub>. All titrations were performed within 48 h of sample collection. For DIC, 0.1 mL of 103% phosphoric acid was injected into the sample vials at 40 °C and reacted for at least 8 h before analysis of headspace CO<sub>2</sub>. Headspace CO<sub>2</sub> was analyzed at the University of Texas at Austin using a Gasbench II coupled to a Thermo MAT-253 isotope ratio mass spectrometer operating in continuous flow mode. The instrument was calibrated for DIC concentration measurements using aqueous sodium bicarbonate standards prepared in house. Reproducibility of measurements of the δ<sup>13</sup>C values of the in-house standard was ±0.15‰ (1σ).

CO<sub>2</sub>, O<sub>2</sub>, Ar and N<sub>2</sub> concentrations were measured at the University of Texas at Austin using an Agilent 7890 gas chromatograph (GC) within about one week after collection. The Agilent 7890 was optimized to separate CO<sub>2</sub>, O<sub>2</sub>, Ar and N<sub>2</sub>. A PAL autosampler was used to transfer 250 μL of sample gas by syringe from the Exetainer vials into the GC injection port. The GC, with cryogenic cooling capability, consists of two GC columns in series separated by a column switching valve. The first column is a 30 m Agilent PoraPLOT Q column and the second column is a 30 m 5 A molecular sieve column. The column valve allows the gas effluent from the PoraPLOT Q column to be directed either through the 5 A molecular sieve column or to bypass the 5 A molecular sieve column and flow directly to the detector. All gas analytes are measured using a thermal conductivity detector (TCD). This GC technique uses a technique referred to as ‘parking’ whereby the CO<sub>2</sub> and ‘air’ peak (air peak consists of unseparated O<sub>2</sub>, N<sub>2</sub> and Ar) are separated on the PoraPLOT Q column at 0 °C. The air peak is eluted onto the 5 A molecular sieve column and ‘parked’ by switching the column valve, effectively closing the loop of 5 A molecular sieve column and isolating the air peak. During this time, the CO<sub>2</sub> is eluted through the TCD and its corresponding peak area measured. After CO<sub>2</sub> measurement, the GC oven is cryogenically cooled to –40 °C, the column valve switched, and the air peak is chromatographically separated to its individual oxygen, argon, and nitrogen components, and the peak areas are measured on the TCD. Separation of O<sub>2</sub> and Ar increased the precision of concentration determinations. Concentra-

tions were determined by ratio to Ar, assuming Ar occurred at atmospheric air concentrations in all samples. This was particularly important for O<sub>2</sub>, for which determination of OR<sub>apparent</sub> required especially high precision (the factor change in concentrations from atmospheric air was much larger for CO<sub>2</sub> than for O<sub>2</sub> concentrations in the samples studied). CO<sub>2</sub>/Ar and O<sub>2</sub>/Ar ratios of the standards at atmospheric concentrations were reproducible within ±0.0001 and ±0.03, respectively (1σ, *n* = 5, a reproducibility of approximately ±0.2% of the measured values, translating to better than ±1 ppmV and ±300 ppmV precision for CO<sub>2</sub> and O<sub>2</sub>, respectively). Two standard gas mixtures calibrated at and purchased from Praxair were used to calibrate measured O<sub>2</sub>/Ar and CO<sub>2</sub>/Ar ratios. Gas mixtures had CO<sub>2</sub>, Ar and O<sub>2</sub> concentrations of 401 ppmV, 0.931%, 20.90% and 20.00%, 0.9305%, 508 ppmV. Differences from atmospheric air in molecular ratios were used to determine OR<sub>apparent</sub> with Eq. (1).

Stable carbon isotope ratios were measured at the University of Texas at Austin using a Thermo MAT 253 isotope ratio mass spectrometer (IRMS) within two to three weeks of collection. CO<sub>2</sub> concentrations measured by the GC were used to determine appropriate size samples for measurement of δ<sup>13</sup>C values of CO<sub>2</sub>. Appropriate-sized aliquots were transferred by valved syringe from each collection vial into newly UHP He-flushed exetainers. The CO<sub>2</sub> in these vials was cryo-focused using a Gasbench II and then introduced to a Thermo Electron 253 IRMS operating in continuous flow mode. Internal laboratory CO<sub>2</sub>-in-air standards, which were analyzed alongside unknowns during each IRMS run, were calibrated against calcium carbonate standards NBS 18, NBS 19 and a CO<sub>2</sub>-in-air standard calibrated at the Stable Isotope Laboratory at CU-INSTAAR in Boulder, Colorado. The δ<sup>13</sup>C value of the internal laboratory standards was reproducible within ±0.1‰. Stable carbon isotope ratios are expressed in the standard delta notation relative to PDB (Pee Dee Belemnite).

Cave-air, soil-gas, and cave drip-water DIC samples were processed for <sup>14</sup>C and δ<sup>13</sup>C analysis at the University of California, Irvine. For gas samples, CO<sub>2</sub> was cryogenically separated from 1 to 2 L glass flasks using vacuum-line extraction. Sample sizes (mgC) were obtained manometrically on the vacuum-line. Drip-water samples were processed using a headspace-extraction method (Gao et al., 2014). In the first step, 30 ml water samples were injected into pre-cleaned, UHP He flushed 60 ml I-Chem septum capped vials and subsequently acidified with 0.5 ml 85% phosphoric acid (H<sub>3</sub>PO<sub>4</sub>). The samples were then shaken and heated at 75 °C for 2 h. In the second step, headspace gases, including CO<sub>2</sub>, were extracted using a syringe and injected into a vacuum line, where they were cryogenically purified before graphitization. Separate aliquots of CO<sub>2</sub> were taken for δ<sup>13</sup>C measurements using a Gasbench coupled with an IRMS (Thermo Fisher Scientific Delta + XL) when total sample size was large enough (>0.3 mg C). Graphite for all AMS measurements was produced from CO<sub>2</sub> using a sealed-tube zinc reduction method (Xu et al., 2007). Graphite was pressed into an aluminum target holder and analyzed for <sup>14</sup>C at the Keck Carbon Cycle Accelerator Mass Spectrometer (KCCAMS) facility

at the University of California, Irvine (Southon et al., 2004; Beverly et al., 2010). All  $^{14}\text{C}$  data are presented according to the conventions in Stuiver and Polach (1977).

### 3.4. Theoretical trends in $\Delta\text{O}_2/\text{Ar}$ vs. $\Delta\text{CO}_2/\text{Ar}$

Trends in  $\Delta\text{O}_2/\text{Ar}$  and  $\Delta\text{CO}_2/\text{Ar}$  expected for respiration, respiration followed by loss of  $\text{CO}_2$  and gain of  $\text{O}_2$  by diffusion (respiration + diffusion), and for exchange between gas and water were calculated to compare with observations. We use a baseline OR of  $1.08 \pm 0.06$  (Hockaday et al., 2009) which overlaps with a number of independent soil respiration OR estimates (Clay and Worrall, 2015a,b; Dilly, 2001). The respiration trend in  $\Delta\text{O}_2/\text{Ar}$  vs.  $\Delta\text{CO}_2/\text{Ar}$  space was plotted as  $\Delta\text{O}_2/\text{Ar} = \Delta\text{CO}_2/\text{Ar}$  (-OR). The respiration + diffusion trend was quantified using diffusion coefficients for  $\text{CO}_2$  and  $\text{O}_2$  in air calculated from (Massman, 1998):

$$D(T,p) = D(0,1) \frac{p_0}{p} \left( \frac{T}{T_0} \right)^{1.81} \quad (2)$$

where  $D(T,p)$  is the diffusion coefficient for the gas of interest at a particular temperature ( $T$ ) and pressure ( $p$ ),  $D(0,1)$  is the diffusion coefficient at reference temperature (273.15 K) and pressure (1 atm),  $T$  and  $p$  are the temperature and pressure of interest (295 K, and 1 atm, respectively). We used  $D(0,1) = 0.138$  and  $0.182 \text{ cm}^2/\text{s}$  for diffusion of  $\text{CO}_2$  and  $\text{O}_2$  in air, respectively (Massman, 1998), resulting in  $D_{\text{CO}_2}$  and  $D_{\text{O}_2}$  equal to 0.152 and  $0.201 \text{ cm}^2/\text{s}$ , respectively. The respiration + diffusion trend was plotted as  $\Delta\text{O}_2/\text{Ar} = \Delta\text{CO}_2/\text{Ar}$  (-OR) ( $D_{\text{CO}_2}/D_{\text{O}_2}$ ), which is derived in the Appendix and has a slope of  $-0.82$ . The trend for exchange between gas and water is defined by the equation  $\Delta\text{O}_2/\text{Ar} = \Delta\text{CO}_2/\text{Ar}$  (-OR<sub>apparent</sub>), where OR<sub>apparent</sub> is the apparent OR resulting from exchange between gas and water (as opposed to actual OR resulting from respiration) and equals 0.042 for a water/cave volume ratio of 1/100 (see Appendix for details).

## 4. RESULTS

### 4.1. Drip water

Within the study interval, drip-water alkalinity had a mean value of  $4.2 \pm 1.1 \text{ meq/L}$  and was higher during the summer than the winter (Table S1). Drip-water pH also varied seasonally with higher values during the winter and lower values during the summer, with a mean of  $7.76 \pm 0.45$  (Table S1). Alkalinity and pH were used to calculate bicarbonate concentrations, which were then used to calculate  $P_{\text{CO}_2\text{sat}}$ , an estimate of the  $p\text{CO}_2$  at which the water last equilibrated with calcite, following Peyraube et al. (2012) with the assumption that activity coefficients equal 1. Values of  $P_{\text{CO}_2\text{sat}}$  also vary seasonally at most drip sites studied, with higher values during the summer (and fall at some sites) than during the winter and spring (Fig. 2).  $P_{\text{CO}_2\text{sat}}$  measured at NBWS, NBBC, ISST and ISLM was higher than maximum measured soil  $\text{CO}_2$  overlying the caves (Fig. 2). Note that this comparison is conservative, as the soil  $\text{CO}_2$  concentrations represented by the

dashed line in Fig. 2 are seasonal and spatial maximum values, and are thus significantly higher than average concentrations (Table S2). Drip-water DIC had lower and less variable  $\delta^{13}\text{C}$  values (mean =  $-13.5 \pm 0.6\text{‰}$ ) at NBWS than at other NB drip sites ( $-9.1 \pm 2.0\text{‰}$  and  $-9.5 \pm 1.3\text{‰}$  for NBCT and NBBC, respectively), supporting the characterization of NBWS as a “direct drip” (following Meyer et al., 2014) that undergoes minimal  $\text{CO}_2$  degassing inside the cave and therefore most accurately reflects the  $\text{CO}_2$  concentration in bedrock fractures above the cave.

### 4.2. Oxidative ratios

The mean Ar concentrations in the caves ( $0.899 \pm 0.06\%$ ,  $1 \sigma$ ,  $n = 61$ ) and soils ( $0.901 \pm 0.02\%$ ,  $1 \sigma$ ,  $n = 217$ ) studied here, are indistinguishable, within the precision of the analytical method used, from that measured in atmospheric air in this study ( $0.904 \pm 0.05\%$ ,  $1 \sigma$ ,  $n = 43$ ). For the samples of atmospheric air, measured Ar concentrations explain 96% of the variance in measured  $\text{O}_2$  concentrations with a slope of 21.1 (for comparison, the accepted  $\text{O}_2/\text{Ar}$  ratio in atmospheric air is 22.4) consistent with substantial effects of variable water vapor contents and/or volumes/pressures of gas samples injected into the GC on measured  $\text{O}_2$  and Ar concentrations. This correlation supports the use of ratios to Ar to account for these effects. We cannot, however, rule out mean deviations in soil gas and cave air from atmospheric Ar concentrations that are smaller than about 20 and 40 ppmV, respectively. This propagates to an uncertainty of  $\pm 0.05$  and 0.1, respectively, on our estimates of best fit OR in addition to the standard error of the regression slopes given below.

$\Delta\text{CO}_2/\text{Ar}$  values and  $\Delta\text{O}_2/\text{Ar}$  values were calculated by comparison with  $\text{CO}_2/\text{Ar}$  and  $\text{O}_2/\text{Ar}$  ratios measured in samples of atmospheric air collected outside the caves on the days of sampling. Atmospheric  $\text{CO}_2/\text{Ar}$  and  $\text{O}_2/\text{Ar}$  values were steady during the period of study (in the atmosphere, mean  $\text{CO}_2/\text{Ar}$  was  $0.0442 \pm 0.0042$  and mean  $\text{O}_2/\text{Ar}$  was  $22.58 \pm 0.16$ ,  $1\sigma$ ,  $n = 56$ ).  $\Delta\text{CO}_2/\text{Ar}$  values in soil gas ranged from 0.0004 to 2.431 (approximately 400–23,000 ppmV  $\text{CO}_2$ ) and from 0.0082 to 2.882 (500–27,000 ppmV  $\text{CO}_2$ ) above NB and IS, respectively (Table S2, Figs. 2 and 3).  $\Delta\text{CO}_2/\text{Ar}$  values in cave air ranged from 0.1162 to 0.9187 (approximately 1500–9000 ppmV  $\text{CO}_2$ ) and from 0.0862 to 0.6955 (1200–7000 ppmV  $\text{CO}_2$ ) in NB and IS, respectively.  $\Delta\text{O}_2/\text{Ar}$  values in soil gas ranged from +0.16 to  $-1.68$  (approximately 21.10–19.38%  $\text{O}_2$ ) and from +1.32 to  $-4.70$  (22.18–16.56%  $\text{O}_2$ ) above NB and IS, respectively.  $\Delta\text{O}_2/\text{Ar}$  values in cave air ranged from  $-0.06$  to  $-0.99$  (approximately 20.89–20.03%  $\text{O}_2$ ) and from  $-0.03$  to  $-1.57$  (20.92–19.48%  $\text{O}_2$ ) in NB and IS, respectively (Table S2, Fig. 3). OR<sub>apparent</sub> values by month were determined as the slope of the best fit line through all the data ( $\Delta\text{O}_2/\text{Ar}$  vs.  $\Delta\text{CO}_2/\text{Ar}$ ) for that month. These monthly OR<sub>apparent</sub> values range from 0.63 to 1.09 and from 0.69 to 1.71 in soils at NB and IS, respectively (Fig. 4). In the caves, these monthly OR<sub>apparent</sub> values range from 0.90 to 1.15 and from 1.31 to 2.35 at NB and IS, respectively. Whereas there was no seasonal variation in OR<sub>apparent</sub> at NB, there

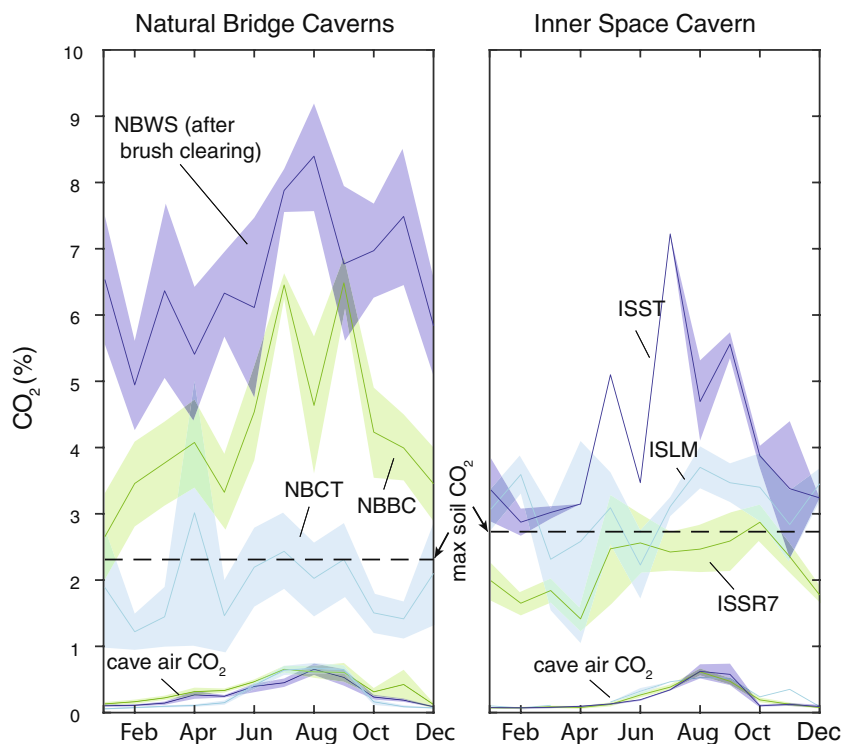


Fig. 2. Vadose zone  $\text{CO}_2$  concentrations in central Texas. Monthly mean and standard error of  $P_{\text{CO}_2, \text{sat}}$  over the entire monitoring interval at each site are shown for drip sites NBWS (2007–2017), NBBC (2007–2017), NBCT (2001–2017), ISST (2013–2017), ISLM (2000–2004 & 2013–2015) and ISSR7 (2009–2017).  $P_{\text{CO}_2, \text{sat}}$  was calculated from the alkalinity and pH of cave drip waters following Peyraube et al. (2012). Dashed horizontal lines indicate the maximum soil  $\text{CO}_2$  concentrations observed during monitoring between 2010 and 2011 (Breecker et al., 2012), 2011–2012 (Meyer et al., 2014) and 2014–2015 (this study). Values of  $P_{\text{CO}_2, \text{sat}}$  at drip sites NBWS, NBBC, ISST and ISLM exceed maximum measured soil  $\text{CO}_2$ , indicating the presence of a subsoil  $\text{CO}_2$  source. The mean and standard error are also shown for cave air  $\text{CO}_2$  concentrations at each site and are an order of magnitude smaller than  $P_{\text{CO}_2, \text{sat}}$ .

were seasonal variations in cave-air  $\text{OR}_{\text{apparent}}$  at IS during the sampling period (Fig. 4). The cave-air  $\text{OR}_{\text{apparent}}$  at IS reached maximum values (2.31–2.35) during August and September, and minimum values of 1.31 in May and 1.60 in October, generally following outside air temperature and cave-air  $\text{pCO}_2$ . There was also a prominent spike in  $\text{OR}_{\text{apparent}}$  in IS soils during September.

Overall cave-air and soil-gas  $\text{OR}_{\text{apparent}}$  values were determined as the slope of the best fit line through all the data ( $\Delta\text{O}_2/\text{Ar}$  vs.  $\Delta\text{CO}_2/\text{Ar}$ ). At both Inner Space and Natural Bridge caverns, soil-gas  $\text{OR}_{\text{apparent}}$  values generally follow the trend expected from theory for respiration + diffusion, whereas cave-air  $\text{OR}_{\text{apparent}}$  values do not (Figs. 3 and 4). Best fit soil-gas  $\text{OR}_{\text{apparent}}$  values are  $0.67 \pm 0.05$  at NB and  $1.01 \pm 0.08$  at IS, as compared with the theoretical respiration + diffusion trend of 0.82. Removing the high September values at IS, the best fit  $\text{OR}_{\text{apparent}}$  in IS soils becomes 0.77, consistent with the respiration + diffusion trend. NB South cave-air  $\text{OR}_{\text{apparent}}$  values align well with the theoretical trend expected for respiration with no subsequent diffusion, whereas IS cave-air  $\text{OR}_{\text{apparent}}$  values tend to be higher than the expected trend for respiration. That is, they plot farther away from the diffusive signature than do NB cave-air data points (Fig. 3). The few NB North cave-air samples (from site NBCT) follow a

trajectory that lies between the respiration trend and the trend defined by IS cave-air samples. Best fit cave-air  $\text{OR}_{\text{apparent}}$  values are  $1.09 \pm 0.06$  at NB South and  $2.40 \pm 0.14$  at IS, as compared with the trend expected for respiration of  $1.08 \pm 0.06$ .

### 4.3. Stable carbon isotope ratios

The  $\delta^{13}\text{C}$  values of soil  $\text{CO}_2$  ranged from  $-21.8$  to  $-9.7\text{‰}$  and from  $-24.9$  to  $-11.7\text{‰}$  at NB and IS, respectively (Table S3). The  $\delta^{13}\text{C}$  values of cave-air  $\text{CO}_2$  ranged from  $-20.0$  to  $-14.4\text{‰}$  and from  $-22.3$  to  $-14.8\text{‰}$  in NB and IS respectively. Although these soil and cave-air  $\text{CO}_2$   $\delta^{13}\text{C}$  values overlap, the radiocarbon activities do not (see Section 4.4) and the oxidative ratios are consistent with diffusion in soils but no net transport by diffusion in NB South cave air. Therefore, it is instructive to use the measured  $\delta^{13}\text{C}$  values along with the  $\text{CO}_2$  concentrations in the gas samples to calculate  $\delta^{13}\text{C}$  values of the carbon source(s) of  $\text{CO}_2$ :  $\delta^{13}\text{C}_r$  (soil) and  $\delta^{13}\text{C}_{\text{bg}}$  (cave) values. The notation  $\delta^{13}\text{C}_r$  is widely used to indicate the  $\delta^{13}\text{C}$  value of respired  $\text{CO}_2$ . We introduce  $\delta^{13}\text{C}_{\text{bg}}$ , which is intended to indicate the weighted mean  $\delta^{13}\text{C}$  value of all potential belowground carbon sources to cave-air  $\text{CO}_2$  (e.g., respired  $\text{CO}_2$ , host rock carbon,  $\text{CO}_2$  degassed from drip water

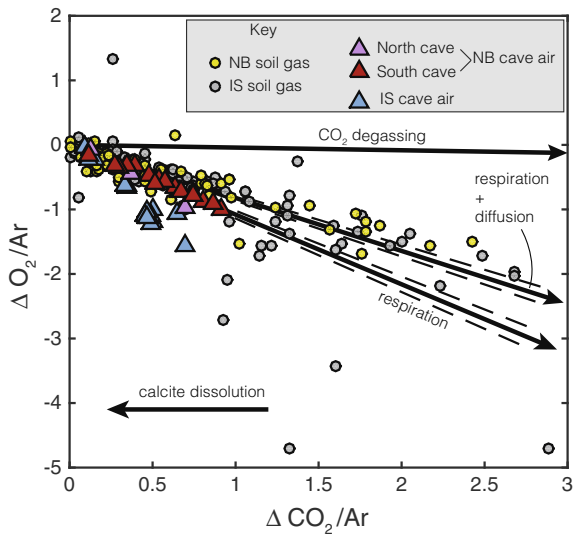


Fig. 3. Molecular ratios ( $\text{CO}_2/\text{Ar}$  and  $\text{O}_2/\text{Ar}$ ) in soil gas and cave air from central Texas.  $\text{CO}_2/\text{Ar}$  and  $\text{O}_2/\text{Ar}$  ratios are plotted as differences from atmospheric air (the origin at upper left on this plot). Respiration consumes  $\text{O}_2$  and produces  $\text{CO}_2$  with an oxidative ratio (OR, the slope of trends on this plot) of  $1.08 \pm 0.06$  (Hockaday et al., 2009), following the trend shown by the “respiration” line. Underground air influenced by respiration and loss of  $\text{CO}_2$ /addition of  $\text{O}_2$  by diffusion should plot along the “respiration + diffusion” trend due to the larger diffusion coefficient for  $\text{O}_2$  than  $\text{CO}_2$  in air. Degassing of  $\text{CO}_2$  from (and ingassing of  $\text{O}_2$  into) seepage water drives cave air to the right along the “ $\text{CO}_2$  degassing” trend. Limestone weathering in closed systems with sufficiently high water/gas volume ratios results in solution of  $\text{CO}_2$  gas into water and thus drives gas compositions directly to the left on this plot along the “calcite dissolution” trend. Soil-gas samples (circles) generally follow the respiration + diffusion trend (with the exception of IS samples collected in September, Fig. 4). NB South cave air samples (red triangles) closely follow the respiration trend. IS cave air samples (blue triangles) plot along a trend suggesting that weathering of limestone in the IS epikarst occurs in a partly closed system.

inside the cave, etc.), in order to emphasize the complexity inherent in cave carbon sources. Monthly soil  $\delta^{13}\text{C}_r$  and cave  $\delta^{13}\text{C}_{bg}$  were determined as the intercept of the best fit line through all the data ( $\delta^{13}\text{C}$  vs.  $1/\text{CO}_2$ , i.e., a Keeling plot; Keeling, 1958) for that month. The Keeling plot approach mathematically unmixes the atmospheric component. For soils, 4.4‰ was subtracted from the Keeling plot y-intercept to account for diffusion, an adjustment supported by the  $\text{OR}_{\text{apparent}}$  values suggesting that soil-gas compositions are modified by diffusion. These soil  $\delta^{13}\text{C}_r$  values ranged from  $-25.9$  to  $-23.5$ ‰ and were generally lower under oak trees than under elm and Ashe juniper trees (Fig. 5). For caves, we considered  $\delta^{13}\text{C}_{bg}$  values calculated as (1) the Keeling plot intercepts and (2) the Keeling plot intercepts minus 4.4‰. Compared with the diffusion-corrected soil-gas  $\delta^{13}\text{C}_r$  values under trees, the Keeling plot intercept cave-air  $\delta^{13}\text{C}_{bg}$  values are 4–5‰ higher whereas the diffusion-corrected cave-air  $\delta^{13}\text{C}_{bg}$  values are similar (Fig. 5).

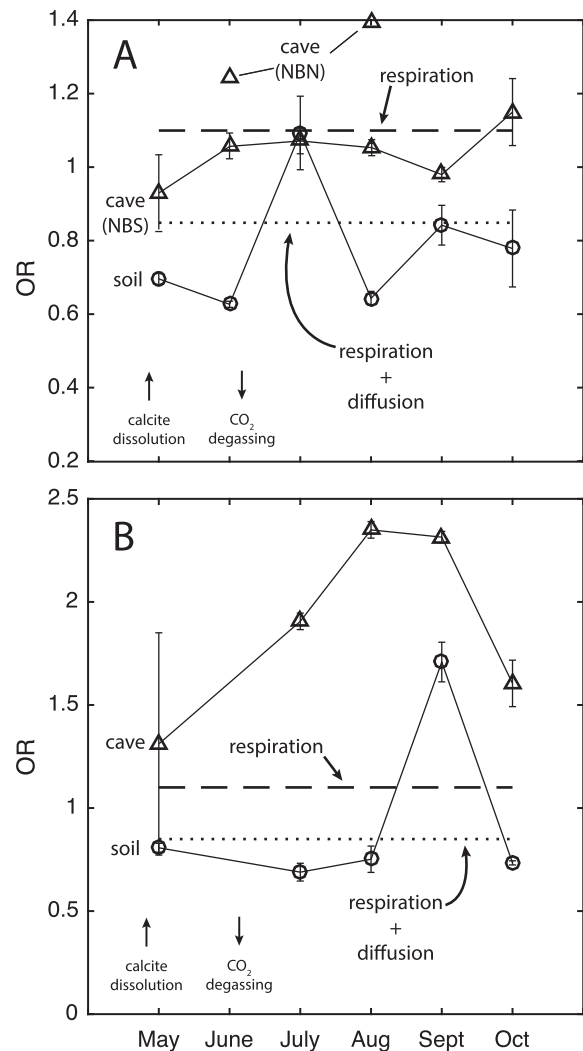


Fig. 4. Time series of cave and soil  $\text{OR}_{\text{apparent}}$ . Values of  $\text{OR}_{\text{apparent}}$  were calculated from the slopes of the best fit lines through the  $\Delta\text{CO}_2/\text{Ar}$  and  $\Delta\text{O}_2/\text{Ar}$  ratios from all sampling sites for each month at (A) NB and (B) IS caverns. The horizontal dashed and dotted lines represent OR expected for respiration and for respiration + diffusion, respectively. Error bars represent standard error of regression lines for each month. Cave air OR values (triangles) follow the respiration trend at NB South (NBS) and vary seasonally at IS. Two individual OR values for NB North (NBN) are also shown, based on the single site that was sampled, NBCT. Soil-gas OR values (circles) approximately follow the respiration + diffusion trend with exception of samples collected in September at IS.

#### 4.4. Radiocarbon activities

At NB, mean values of fraction modern carbon (FMC) are  $1.0248 \pm 0.0420$  ( $n = 4$ ),  $0.9836 \pm 0.0104$  ( $n = 6$ ) and  $0.8205 \pm 0.1452$  ( $n = 4$ ) for soil  $\text{CO}_2$ , cave-air  $\text{CO}_2$  and drip-water DIC, respectively (Table 1). Cave-air  $\text{CO}_2$  FMC values are lower than most of the soil  $\text{CO}_2$  FMC values. Cave-air  $\text{CO}_2$  samples have radiocarbon activities consistent with an organic carbon source greater than 100 years old, whereas most of the soil  $\text{CO}_2$  samples have radiocar-

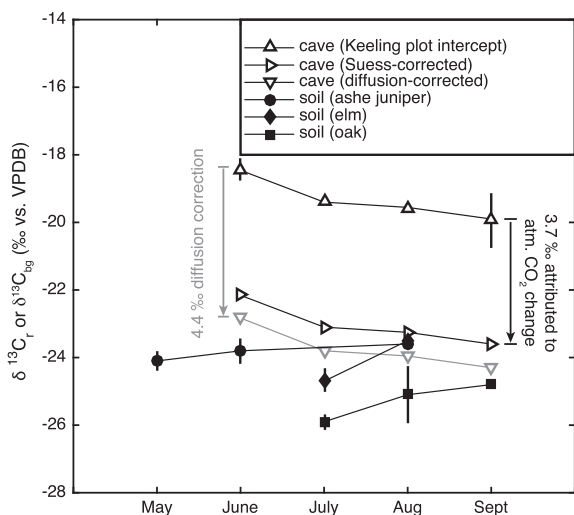


Fig. 5. Best fit  $\delta^{13}\text{C}_r$  (soil) and  $\delta^{13}\text{C}_{bg}$  (cave) values versus sampling month at Natural Bridge Caverns South. Cave air  $\delta^{13}\text{C}_{bg}$  values calculated from Keeling plot intercepts are 4–5‰ higher than soil-gas  $\delta^{13}\text{C}_r$  values (also from Keeling plot intercepts and with an additional diffusion-correction) under trees. The standard error of the regression intercept is shown where it is larger than the symbols. Breecker et al. (2012) and Meyer et al. (2014) suggested correcting cave air  $\delta^{13}\text{C}_{bg}$  values for diffusion (gray arrow and triangles), bringing them into agreement with the soil-gas  $\delta^{13}\text{C}_r$  values. The molecular data, however, indicate that NB cave air has not lost  $\text{CO}_2$  by diffusion (Fig. 4A). An alternative explanation for the elevated cave air  $\delta^{13}\text{C}_{bg}$  values that we propose here supposes that cave air  $\text{CO}_2$  is primarily sourced from >100-year-old organic matter in the epikarst, which has  $\delta^{13}\text{C}$  values approximately 3.7‰ higher than soil-respired  $\text{CO}_2$ . Higher  $\delta^{13}\text{C}$  values of aged organic matter are consistent with effects of anthropogenic atmospheric  $\text{CO}_2$  changes including 1) decreases in the  $\delta^{13}\text{C}$  value of atmospheric  $\text{CO}_2$  (2‰; Center for Carbon Dioxide Information and Analysis; Francey et al., 1999) and 2) increases in atmospheric  $p\text{CO}_2$  (Etheridge et al., 1996; Keeling and Whorf, 2005). The increase in atmospheric  $p\text{CO}_2$  over the past century has been suggested to result in a 1.7‰ decrease in  $\delta^{13}\text{C}$  values of  $\text{C}_3$  plants (Schubert and Jahren, 2012), resulting in a total 3.7‰ shift attributable to atmospheric  $\text{CO}_2$  change. Radiocarbon activities (Table 1) support an aged organic carbon source for cave air  $\text{CO}_2$ . Alternative explanations for elevated cave air  $\delta^{13}\text{C}_{bg}$  values are discussed in the text.

bon activities that reflect the presence of bomb carbon ( $\text{FMC} > 1$ ). One of the soil-gas samples (Elm 1a) has an FMC value (0.9629) similar to cave-air  $\text{CO}_2$ . Drip-water FMC values are variable. One drip-water sample (NBWS) has an FMC value (0.9994) similar to cave-air  $\text{CO}_2$  whereas the other drip-water samples have substantially lower FMC values.

## 5. DISCUSSION

The observation that  $P_{\text{CO}_2, \text{sat}}$  at a number of drip sites exceeds maximum observed soil  $\text{CO}_2$  concentrations (Fig. 2) indicates that there is a subsurface carbon source in the central Texas karst. Similar conclusions have been made with regard to other karst regions (e.g., Atkinson, 1977; Faimon et al., 2012). We investigate this subsurface carbon

source, with a focus on its radiocarbon activity and  $\delta^{13}\text{C}$  values.

The first step toward investigating the subsurface carbon source is to assess which subsurface processes might influence the carbon isotope compositions of the cave-air  $\text{CO}_2$ . We ask, for instance, does diffusion affect the  $\delta^{13}\text{C}$  values of  $\text{CO}_2$  in cave air? Is there a host rock contribution to the carbon in cave-air  $\text{CO}_2$ ? If our objective is to learn something about the subsurface organic carbon source for  $\text{CO}_2$ , then we need to account for such processes. We introduce the use of  $\text{OR}_{\text{apparent}}$  for this purpose.

### 5.1. Constraints from $\text{OR}_{\text{apparent}}$ in natural bridge south caverns

NB south cave-air  $\text{OR}_{\text{apparent}}$  values suggest that respiration is the only subsurface process controlling the carbon isotope compositions of cave-air  $\text{CO}_2$ . Based on the relationships shown in Fig. 3, the simplest explanation for the observed values of  $\text{OR}_{\text{apparent}}$  at NB South is that 1) respiration occurs in a region with large enough gas/water volume ratios such that host rock dissolution occurs under open-system conditions and thus does not affect the composition of the gas, 2)  $\text{CO}_2$  degassing from drip water is an insignificant contribution to cave-air  $\text{CO}_2$  and 3) the composition of the cave air has not been modified by diffusion. This explanation involving the absence of a substantial flux from  $\text{CO}_2$  degassing from drip water into cave air is in agreement with the study of metal concentrations in drip waters in NB (Wong and Banner, 2010) and in Jack's Cave in Arkansas (Knierim et al., 2015).

NB South  $\text{OR}_{\text{apparent}}$  values suggest that either  $\text{CO}_2$  is respired inside the cave or that respiration occurs somewhere else, such as the bedrock fracture network, and the gas is then advected into the cave. The effect of human respiration inside NBS, NBN, and IS caverns is considered to be small, based on lack of changes in  $\text{CO}_2$  as tour groups pass as well as with monthly changes in visitation (Cowan, 2010), the similar  $\delta^{13}\text{C}$  values of cave-air  $\text{CO}_2$  observed in nearby wild caves (Breecker et al., 2012), and the low radiocarbon activities of cave-air  $\text{CO}_2$  (Table 1). We prefer the latter fracture-advection explanation for these reasons, but also because bedrock fractures typically have higher  $\text{CO}_2$  concentrations than air inside cave passages (Atkinson, 1977; Ek and Gewalt, 1985; Baldini et al., 2006; Benavente et al., 2010). Indeed, there is also evidence from central Texas for higher  $\text{CO}_2$  concentrations in bedrock fractures than in cave passages. Sustained air flow for up to nine consecutive hours out of the entrances of Whirlpool and Maple Run Caves was associated with increases in cave-air  $\text{CO}_2$  concentrations (Cowan, 2010). The volume of air passing through the cave entrances was 1x and 15x the volume of the known cave passages in Whirlpool and Maple Run, respectively. This suggests that air advects from fractures with elevated  $\text{CO}_2$  concentrations through cave passages. Advection of  $\text{CO}_2$  into central Texas caves is additionally supported by the observation of high cave-air  $p\text{CO}_2$  in Whirlpool, a cave with few active drips compared with IS and NB caverns (Cowan, 2010; Cowan et al., 2013). The consistently observed  $\text{CO}_2$  concen-

Table 1  
Radiocarbon data.

| Sample type          | Cave name | Sample                     | Date collected | Date measured | Fraction modern | ±      | <sup>14</sup> C age (yBP) |
|----------------------|-----------|----------------------------|----------------|---------------|-----------------|--------|---------------------------|
| Soil CO <sub>2</sub> | NB        | NB Ashe 1A                 | 27-06-2015     | 01-08-2015    | 1.0437          | 0.0017 | Modern                    |
|                      | NB        | NB Elm 1A                  | 27-06-2015     | 01-08-2015    | 0.9629          | 0.0016 | 305                       |
|                      | NB        | NB Oak 1A                  | 27-06-2015     | 01-08-2015    | 1.0363          | 0.0017 | Modern                    |
|                      | NB        | NBS1                       | 24-02-2013     | 09-04-2013    | 1.0561          | 0.0019 | Modern                    |
|                      | NB        | Mean soil CO <sub>2</sub>  |                |               | <b>1.0248</b>   |        |                           |
|                      | NB        | stdev soil CO <sub>2</sub> |                |               | <b>0.0420</b>   |        |                           |
| Cave air             | NB        | NBVC                       | 27-06-2015     | 01-08-2015    | 0.9915          | 0.0016 | 70                        |
|                      | NB        | NBBC                       | 27-06-2015     | 01-08-2015    | 0.9891          | 0.0016 | 90                        |
|                      | NB        | NBCT (north)               | 27-06-2015     | 01-08-2015    | 0.9719          | 0.0017 | 230                       |
|                      | NB        | NBSB (north)               | 27-06-2015     | 01-08-2015    | 0.9867          | 0.0016 | 105                       |
|                      | NB        | NBFE                       | 27-06-2015     | 01-08-2015    | 0.9932          | 0.0018 | 55                        |
|                      | NB        | NBFT                       | 24-02-2013     | 09-04-2013    | 0.9691          | 0.0015 | 250                       |
|                      | NB        | Mean cave air              |                |               | <b>0.9836</b>   |        |                           |
|                      | NB        | stdev cave air             |                |               | <b>0.0104</b>   |        |                           |
| Drip-water DIC       | NB        | NBBC                       | 26-02-2013     | 14-08-2013    | 0.7028          | 0.0014 | 2835                      |
|                      | NB        | NBBC 2                     | 26-02-2013     | 14-08-2013    | 0.7018          | 0.0012 | 2845                      |
|                      | NB        | NBCT                       | 26-02-2013     | 14-08-2013    | 0.8781          | 0.0015 | 1045                      |
|                      | NB        | NBWS                       | 26-02-2013     | 14-08-2013    | 0.9994          | 0.0018 | 5                         |
|                      | NB        | Mean drip water            |                |               | <b>0.8205</b>   |        |                           |
|                      | NB        | stdev drip water           |                |               | <b>0.1452</b>   |        |                           |
| Soil gas             | IS        | IS Elm                     | 23-03-2013     | 14-08-2013    | 0.9433          | 0.0017 | 470                       |
| Cave air             | IS        | ISLM                       | 23-03-2013     | 14-08-2013    | 0.9500          | 0.0016 | 410                       |
| Drip-water DIC       | IS        | ISST indirect              | 23-03-2013     | 14-08-2013    | 0.9021          | 0.0016 | 830                       |
|                      | IS        | ISSR7                      | 23-03-2013     | 14-08-2013    | 0.8619          | 0.0017 | 1195                      |
|                      | IS        | ISLM                       | 23-03-2013     | 14-08-2013    | 0.9756          | 0.0017 | 200                       |
|                      |           |                            |                |               |                 |        |                           |

tration gradient between cave air and fractures suggests the CO<sub>2</sub> source is in the fractures. A CO<sub>2</sub> source within bedrock fractures has support from a number of recent studies in various caves (e.g., Noronha et al., 2015; Matthey et al., 2016; McDonough et al., 2016). Intact, living tree roots as well as decomposing root fragments that have been observed in bedrock fractures provide a reasonable carbon source thought to control respiration even below 1 m in deep soils of the Eastern Amazon (Davidson and Trumbore, 1995). Moreover, roots are commonly observed penetrating through cave ceilings (e.g., Jackson et al., 1999; Baldini et al., 2006; Frisia et al., 2011). At NB, clearing Ashe juniper trees above the cave resulted in a decrease in cave-air CO<sub>2</sub> concentrations, suggesting tree roots, probably extending into bedrock fractures, are a substantial CO<sub>2</sub> source (Wong and Banner, 2010). Indeed, we have observed tree roots several mm in diameter in the bedrock above Inner Space Cavern during a pilot coring operation that reached a depth of two meters. Another possible subsoil CO<sub>2</sub> source is oxidation of DOC at the water table (e.g., Whitaker and Smart, 2007; Benavente et al., 2010).

There is also substantial evidence for a physical connection between and advection of gases through bedrock fractures and cave passages, which supports the interpretation that CO<sub>2</sub> is advected as a gas into the caves studied. Cowan's (2010) study of the volume of air flow out of cave entrances supports this idea as does the similar observation in Cueva de Asiul that cave-air CO<sub>2</sub> concentrations increase when atmospheric pressure decreases (Smith et al., 2015). In addition, several studies have demonstrated extensive

ventilation in caves with no known unsealed surface entrances (Spötl et al., 2005; Frisia et al., 2011; Garcia-Anton et al., 2014) and advection throughout the caves and fractures in the Rock of Gibraltar is now well-established (Matthey et al., 2016), suggesting that advection of gases through bedrock fractures is a regular occurrence in many karst regions. Covington (2015) provides theoretical support for these observations, concluding that advection dominates CO<sub>2</sub> transport into caves, even when fractures are thin and span a small elevation difference between their highest and lowest points.

It is possible that the continuously running ventilation fan in NB South pulls large volumes of gas through the bedrock fractures feeding gas into the cave, resulting in an open system. Indeed, OR<sub>apparent</sub> decreases with increasing fan usage (from IS to NB North to NB South, Figs. 3 and 4). It is also possible that the fractures through which gas advects into NB South constitute a naturally open system. Regardless, respiration in bedrock fractures followed by advection of gas into the cave is the simplest explanation that accounts for the results (Figs. 3 and 4). We recognize that the OR<sub>apparent</sub> values at NB South do not theoretically preclude more complicated scenarios involving CO<sub>2</sub> removal from the gas by calcite dissolution followed by return of CO<sub>2</sub> by degassing from drip water. We simply suggest that such scenarios are unlikely because they would require a fortuitous balance between CO<sub>2</sub> consumed by calcite dissolution and CO<sub>2</sub> returned by degassing, such that the gas composition returns to the respiration trend (Figs. 3 and 4).

## 5.2. Additional applications of $OR_{\text{apparent}}$

Inner Space cave-air  $OR_{\text{apparent}}$  values suggest that host rock dissolution does influence the composition of cave air (Fig. 3). This suggests that exchange with the above-ground atmosphere is slow enough (closed system) and the gas/water volume ratio is small enough that host rock dissolution reduces the  $CO_2$  concentration in the gas. This results in a molecular ratio trend consistent with limestone dissolution and perhaps a measurable limestone carbon component in cave-air  $CO_2$ .

It would be interesting to quantitatively consider  $OR_{\text{apparent}}$  along with  $\delta^{13}C$  values and radiocarbon activities of both cave-air  $CO_2$  and drip water. Models exist for simulating variations in  $\delta^{13}C$  values and radiocarbon activities in drip waters (e.g., Fohlmeister et al., 2011). Addition of the composition of cave air, including  $OR_{\text{apparent}}$ , to these models would provide additional constraints that would be helpful for isolating the effects of individual processes of interest, such as separating respiration of aged organic carbon from dissolution of the host rock. Such a model would provide insight into the seasonal change in  $OR_{\text{apparent}}$  observed in IS (Fig. 4B). It could also be used to quantify a more complicated scenario to explain the respiration trend in NB South, involving both  $CO_2$  degassing and host rock dissolution, as opposed to simply respiration in open-system epikarst fractures.

## 5.3. The carbon isotope compositions of the subsoil $CO_2$ source

Our primary objective here is to take advantage of the relatively simple subsurface system at NB South to investigate the subsoil organic carbon  $CO_2$  source. If air masses in NB South have not lost  $CO_2$  by diffusion, as indicated by  $OR_{\text{apparent}}$ , then the Keeling plot intercepts should accurately characterize the  $\delta^{13}C$  value of their carbon source. Why, then, are the cave-air  $\delta^{13}C_{\text{bg}}$  values so much higher than  $\delta^{13}C$  values of soil-respired  $CO_2$  (Fig. 5)? This is not likely explained by a substantial limestone carbon contribution to cave-air  $CO_2$  because the values of  $OR_{\text{apparent}}$  in NB South suggest an open system in which gas composition is not influenced by host rock dissolution. While it is theoretically possible that the combined effects of host rock dissolution and  $CO_2$  degassing on  $OR_{\text{apparent}}$  values have entirely canceled each other out to clearly and consistently yield a respiration trend, the chance of such coincidental results is quite low. Instead, we suggest that the cave-air  $CO_2$  source is aged organic carbon in the vadose zone bedrock fractures that has  $\delta^{13}C$  values that are higher than those of the younger, labile soil organic matter that dominates the soil  $\delta^{13}C_r$  signal. The radiocarbon activities indeed support an older organic carbon source for cave-air  $CO_2$  than for soil  $CO_2$  (Table 1), which is consistent with the results of previous studies (Oster et al., 2010; Breecker et al., 2012; Noronha et al., 2015).

There are several reasons why organic carbon that is >100 years old would have higher  $\delta^{13}C$  values than organic carbon that is less than a couple of decades old. First, there could be a component of organic carbon from  $C_4$  plants in

the subsoil, as there are  $C_4$  plants above NB (Breecker et al., 2012; Meyer et al., 2014). We think this is unlikely given the predominance of tree roots in the subsoil vadose zone, but we cannot entirely preclude this possibility. Second, it is possible that the  $\delta^{13}C$  value of the organic carbon source for NB cave-air  $CO_2$  increased above its original, plant-derived value due to decomposition, which is the mechanism that has been used to explain the down-profile increase in  $\delta^{13}C$  values of organic matter characteristic of well-drained soils (Natelhoffer and Fry, 1988; Balesdent et al., 1993; Wynn et al., 2005; but see Breecker et al., 2015). Third, the  $\delta^{13}C$  value of atmospheric  $CO_2$  has decreased by 2‰ over the past century as a result of the burning of fossil fuels (Center for Carbon Dioxide Information and Analysis; Francey et al., 1999). Fourth, the partial pressure of atmospheric  $CO_2$  has increased by >100 ppmV over the past century (Etheridge et al., 1996; Keeling and Whorf, 2005). Recent studies suggest that the magnitude of carbon isotope fractionation by  $C_3$  plants during photosynthesis increases with atmospheric  $pCO_2$  (Schubert and Jahren, 2012; Frank et al., 2015) and that this signal is transferred to caves (Wong and Breecker, 2015; Breecker, 2017). This effect may have resulted in a decrease in the  $\delta^{13}C$  value of  $C_3$  plants by as much as 1.7‰, all else being equal, over the past century. Together, the magnitude of the atmospheric  $CO_2$ -driven effects sum to 3.7‰, which may explain the signal we see in the comparison of soil (younger and thus lower  $\delta^{13}C$ )  $\delta^{13}C_r$  and cave (older and thus higher  $\delta^{13}C$ )  $\delta^{13}C_{\text{bg}}$  values (Fig. 4). This idea can be tested by developing tree ring  $\delta^{13}C$  records from this region. Regardless, the radiocarbon activities considered along with the values of  $OR_{\text{apparent}}$  support the conclusion from aqueous geochemistry that NB cave-air  $CO_2$  is not sourced from soils overlying the cave.

One question that arises is whether our interpretations relevant to the carbon source for cave-air  $CO_2$  also apply to carbon in drip-water DIC and thus speleothem calcite. Relevant to this question is the observation that  $P_{CO_2\text{sat}}$  varies seasonally in most of the drips studied (Fig. 2). We discount substantial prior calcite precipitation as a control on  $P_{CO_2\text{sat}}$  given the relatively constant  $\delta^{13}C$  values of DIC in the ‘direct’ drips studied here (Meyer et al., 2014; this study). The seasonal variation in  $P_{CO_2\text{sat}}$  also cannot be explained by seasonal variations in soil  $CO_2$  concentrations, even at the drip sites for which  $P_{CO_2\text{sat}}$  values are similar to soil  $CO_2$  concentrations. Soil  $CO_2$  concentrations have more complex variability than does  $P_{CO_2\text{sat}}$ . For instance, there can be multiple maxima and minima in soil  $CO_2$  throughout the year (typically higher values in spring and fall and lower values in later summer and winter) likely due to temperature and moisture limitation of soil respiration at different times of year (Breecker et al., 2012; Meyer et al., 2014).  $P_{CO_2\text{sat}}$  variations are much more similar to the annual cycle in cave-air  $pCO_2$ , with some potential leads and lags at some of the sites (Fig. 2). Furthermore, drip waters in these caves are well mixed, with a narrow range of  $\delta^{18}O$  values that are similar to those of mean annual precipitation (Pape et al., 2010). Thus, any seasonally variable soil  $CO_2$  signal in seepage waters would be smoothed by mixing before reaching the caves. We therefore suggest that

the seasonal variations in  $P_{\text{CO}_2, \text{sat}}$  are controlled by variations in the  $\text{CO}_2$  concentrations in the bedrock fractures routing water to these caves. This, in turn, suggests that these water-routing fractures ventilate seasonally and are therefore either the same fractures that route gas into the caves or exchange carbon with those gas-routing fractures. Either way, the observations suggest that exchange occurs in the subsoil vadose zone between seepage waters and the gas-filled fracture volume and that this exchange overprints the soil signal and controls the chemical and isotopic compositions of speleothems. Despite this exchange, there are certainly some seepage waters that do not attain isotopic equilibrium with  $\text{CO}_2$  in the fractures routing gas into NB South. The absence of isotopic equilibrium despite some degree of exchange is clear from the radiocarbon activities and  $\delta^{13}\text{C}$  values of drip water at NBBC, which are consistent with a host rock contribution that is not observed in the cave-air  $\text{CO}_2$ . Therefore, it is possible that the composition of the subsoil organic carbon source is variable among drip sites and that the source we characterize using cave-air  $\text{CO}_2$  is a weighted average. For instance, radiocarbon activities and  $\delta^{13}\text{C}$  values of DIC at drip site NBWS are consistent with a carbon source that is slightly younger ( $\text{FMC} = 0.9994$ ) and has lower  $\delta^{13}\text{C}$  values ( $\delta^{13}\text{C}$  values of  $\text{CO}_2$  in equilibrium with the measured DIC  $\delta^{13}\text{C}$  values are approximately  $-21\text{‰}$ ) than the carbon source for NB South cave-air  $\text{CO}_2$  ( $\text{FMC} = 0.9836$ ,  $\delta^{13}\text{C} = -19$  to  $-20\text{‰}$ ).

Taken together, the data we report suggest that carbon in speleothem calcite in the caves we studied comes from  $\text{CO}_2$  respired in bedrock fractures (Fig. 6), not in soils as conceptualized by the canonical model. We therefore suggest that interpretation of speleothem  $\delta^{13}\text{C}$  values does not necessarily require consideration of carbon isotope fractionation by diffusion (Breecker et al., 2012). If soil-respired  $\text{CO}_2$  is a substantial source of carbon in speleothem calcite where/when soil is thicker and perhaps where/when roots do not penetrate below the bottom of the soil, then carbon isotope fractionation during diffusion may influence speleothem  $\delta^{13}\text{C}$  values. The occurrence or absence of  $\text{CO}_2$  escape by diffusion, and the associated carbon isotope fractionation, is a potential factor influencing speleothem  $\delta^{13}\text{C}$  values that to our knowledge has not been considered, but could be substantial (up to 4.4‰). All else being equal, a greater proportion of soil versus bedrock fracture-respired carbon in speleothem calcite would result in higher  $\delta^{13}\text{C}$  values. This effect could, however, be somewhat mitigated if subsoil organic carbon with higher  $\delta^{13}\text{C}$  values than soil organic carbon (as suggested by this study, Fig. 5) is a persistent feature through time in karst (e.g. due to decomposition).

## 6. CONCLUSIONS

We introduce the use of the oxidative ratio to help understand the belowground carbon cycle in karst regions.

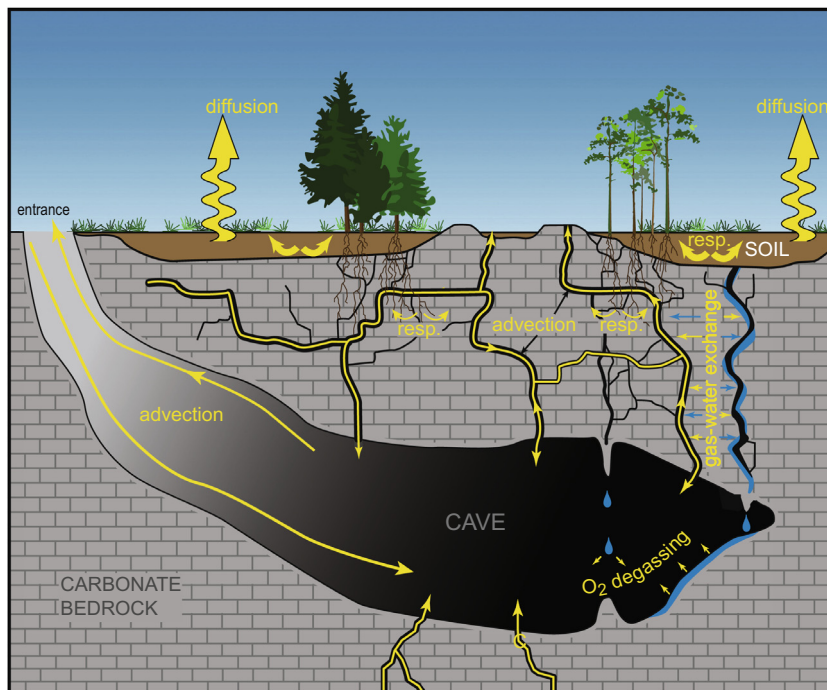


Fig. 6. Conceptual model for subsurface carbon cycling in karst.  $\text{CO}_2$  respired in soils (concave upward curving arrows) is transported by diffusion into the atmosphere (thick, yellow wavy arrows).  $\text{CO}_2$  respired in bedrock fractures is transported by advection into caves and atmosphere (thin yellow arrows). In some caves,  $\text{CO}_2$  enters caves from beneath as shown by yellow arrows entering the floor of the cave. The flux of  $\text{CO}_2$  degassing from seepage waters (blue) into the cave is substantially smaller than the flux of  $\text{CO}_2$  advected as a gas (as represented by yellow arrow size). Exchange between seepage waters and air in bedrock fractures occurs in the subsoil vadose zone. Ventilation through the cave entrance is also shown schematically and can occur by multiple mechanisms with various flow geometries in natural caves.

Measurements of  $OR_{\text{apparent}}$  in cave air can help identify the effects of carbonate rock dissolution,  $CO_2$  degassing from seepage waters and net transfer of gases by diffusion. OR is especially useful when considered alongside measurements of radiocarbon and stable carbon isotope compositions of  $CO_2$ . Mathematical models calculating these three measurable ratios would help quantify belowground variables such as the water content of the epikarst and the fraction of carbonate rock carbon in drip water and in cave-air  $CO_2$ .

The evidence reported here indicates that there is a centuries-old, subsoil organic carbon source in central Texas karst to cave air  $CO_2$ , drip water DIC, and speleothems. Moreover, soil-respired  $CO_2$  is not a dominant source (<50% comparing max. soil  $pCO_2$  with minimum NBWS  $P_{CO_2\text{-sat}}$ ). The soils above the caves studied here are quite thin (~30 cm) in comparison with the depth of the caves themselves (~10 m) and from this perspective, a subsoil carbon source for cave air  $CO_2$  seems quite reasonable. Soil respiration may be a more important carbon source to caves where soils are thicker and/or where roots do not penetrate below the soil. However, given that soils on karst are typically quite thin, a subsoil carbon source may be the rule for karst rather than the exception. Another consideration is that the temperature in the bedrock fractures above the caves studied here is relatively high; respiration in bedrock fractures may contribute a smaller fraction of carbon to cave air  $CO_2$  in colder climates where temperatures are high enough to stimulate substantial respiration only in the soil during the growing season. It is also possible that advection of air by the ventilation fans oxygenates the bedrock fractures above Natural Bridge Caverns, resulting in artificially elevated subsoil respiration rates. Similar studies of other karst regions (e.g. thick soils, colder climates, caves with demonstrably natural open-system fracture networks) are required to address these uncertainties. We nonetheless suggest that given the results of this and other recent studies (Noronha et al., 2015; Matthey et al., 2016; McDonough et al., 2016), it is perhaps time to update the conceptual models for speleothem formation and subsurface carbon cycling to recognize what Atkinson first proposed 40 years ago - that organic carbon in bedrock fractures is the dominant source of carbon for cave air  $CO_2$  and for speleothems in some, and perhaps most, karst regions.

#### ACKNOWLEDGEMENTS

The authors thank the owners, management and staff at Natural Bridge Caverns and Inner Space Cavern, as well as the many UT Austin students in the cave research group who participated in data collection. We also thank P.-Y. Jeannin for helpful discussion, and our three anonymous reviewers whose thoughtful input helped us to improve this manuscript. We are grateful for the support of the Second Mr. and Mrs. Charles E. Yager Professorship and the Fred M. Bullard Professorship of the Geology Foundation at UT Austin. Funding was provided by NSF DUE 1154569, NSF EAR 1451718, NSF AGS 1518541, NSF EAR 1124514 and NSF EAR 1452024.

#### APPENDIX A

The derivation for the equation for the respiration + diffusion trend in  $\Delta O_2/Ar$  vs.  $\Delta CO_2/Ar$  space is as follows. We start with the equations for the concentration of  $O_2$  and  $CO_2$  concentrations as a function of depth ( $z$ ):

$$O_{2(\text{soil})} = O_{2(\text{atm})} + \frac{-P_{o(O_2)}(z_0)^2}{D_{O_2}} (1 - e^{-\frac{z}{z_0}}) \quad (\text{A1})$$

$$CO_{2(\text{soil})} = CO_{2(\text{atm})} + \frac{P_{o(CO_2)}(z_0)^2}{D_{CO_2}} (1 - e^{-\frac{z}{z_0}}) \quad (\text{A2})$$

where  $P_o$  the respiration rate at the soil surface (production of  $CO_2$  and consumption of  $O_2$ ),  $z_0$  is the e-folding depth describing the exponential decrease in respiration rates with depth and the subscripts 'soil' and 'atm' refer to gas concentrations in the soil pore spaces and in atmospheric air, respectively. These equations are the steady state solutions to differential equations for changes in concentration with time assuming diffusion and exponentially decreasing respiration ( $P$ ) with depth (Hesterberg and Siegenthaler, 1991):

$$P(z) = P_o e^{-\frac{z}{z_0}} \quad (\text{A3})$$

The derivation could be carried out with any expression for respiration as a function of depth. The use of the same value of  $z_0$  for  $CO_2$  production and  $O_2$  consumption by respiration is equivalent to assuming that OR for respiration does not change with depth in the soil. Rearranging and combining Eqs. (A1) and (A2), we get:

$$\begin{aligned} \frac{\Delta O_2/Ar}{\Delta CO_2/Ar} &\approx \frac{\Delta O_2}{\Delta CO_2} = \frac{O_{2(\text{atm})} - O_{2(\text{soil})}}{CO_{2(\text{soil})} - CO_{2(\text{atm})}} \\ &= \frac{\frac{P_{o(O_2)}(z_0)^2}{D_{O_2}} (1 - e^{-\frac{z}{z_0}})}{\frac{P_{o(CO_2)}(z_0)^2}{D_{CO_2}} (1 - e^{-\frac{z}{z_0}})} = \frac{P_{o(O_2)}}{P_{o(CO_2)}} \left( \frac{D_{CO_2}}{D_{O_2}} \right) \end{aligned} \quad (\text{A4})$$

Recognizing that

$$\frac{P_{o(O_2)}}{P_{o(CO_2)}} = OR \quad (\text{A5})$$

because the rate of  $O_2$  consumption divided by the rate of  $CO_2$  production gives the moles of  $O_2$  consumed per mole of  $CO_2$  produced (i.e. OR).

Substituting (A5) into (A4) and rearranging, we get the equation for the respiration + diffusion line:

$$\Delta O_2/Ar = \Delta CO_2/Ar (OR) \left( \frac{D_{CO_2}}{D_{O_2}} \right) \quad (\text{A6})$$

The derivation of the equation for the exchange between gas and water trend in  $\Delta O_2/Ar$  space vs.  $\Delta CO_2/Ar$  is as follows. Conceptually, we start with cave-air  $pCO_2$  and  $pO_2$  equal to atmospheric values and then consider how the cave-air values would change if cave air equilibrated with drip water that had previously equilibrated with soil or epikarst air with  $pCO_2$  higher and  $pO_2$  lower than atmospheric air (due to respiration). We have three constraints on this system, which we combine to derive the equation of interest. The first constraint is:

$$CO_{2,T} = \frac{pCO_{2,atm}(V_{cave})}{RT} + pCO_{2,epikarst}(K_H)(V_w) \quad (\text{A7})$$

where  $V$  is volume, the subscript ‘w’ refers to water and  $K_H$  is Henry’s Law constant for  $\text{CO}_2$ . Eq. (A7) sums  $\text{CO}_2$  initially in cave air (at atmospheric concentration) and  $\text{CO}_2$  initially in seepage water entering the cave. The second constraint is:

$$\text{CO}_{2,T} = \frac{p\text{CO}_{2,cave}(V_{cave})}{RT} + \text{CO}_{2,w}(V_w) \quad (\text{A8})$$

which sums  $\text{CO}_2$  in cave air and in water after equilibration inside the cave. In Eq. (A8), we can use the third constraint:

$$\frac{\text{CO}_{2,w}}{p\text{CO}_{2,cave}} = K_H. \quad (\text{A9})$$

We solve this system of equations for  $p\text{CO}_{2,cave}$ . First, by rearranging (A9) and substituting into (A8), we get:

$$\text{CO}_{2,T} = \frac{p\text{CO}_{2,cave}(V_{cave})}{RT} + p\text{CO}_{2,cave}(K_H)(V_w) \quad (\text{A10})$$

Substituting into (A10) in to (A7) and rearranging, we get:

$$p\text{CO}_{2,cave} = \frac{\frac{p\text{CO}_{2,atm}(V_{cave})}{RT} + p\text{CO}_{2,epikarst}(K_H)(V_w)}{\frac{V_{cave}}{RT} + (K_H)(V_w)} \quad (\text{A11})$$

Likewise,

$$p\text{O}_{2,cave} = \frac{\frac{p\text{O}_{2,atm}(V_{cave})}{RT} + p\text{O}_{2,epikarst}(K_{H,\text{O}_2})(V_w)}{\frac{V_{cave}}{RT} + (K_{H,\text{O}_2})(V_w)} \quad (\text{A12})$$

The apparent OR is then given by:

$$\text{OR}_{\text{apparent}} = \frac{p\text{O}_{2,atm} - p\text{O}_{2,cave}}{p\text{CO}_{2,cave} - p\text{CO}_{2,atm}} \quad (\text{A13})$$

into which Eqs. (A11) and (A12) can be substituted in order to calculate  $\text{OR}_{\text{apparent}}$ , which is equivalent to the slope of the “exchange with seepage water” trend in Fig. 2.

## APPENDIX B. SUPPLEMENTARY MATERIAL

Supplementary data associated with this article can be found, in the online version, at <http://dx.doi.org/10.1016/j.gca.2017.08.017>.

## REFERENCES

- Amiotte Suchet P., Probst J. L. and Ludwig W. (2003) Worldwide distribution of continental rock lithology: Implications for the atmospheric/soil  $\text{CO}_2$  uptake by continental weathering and alkalinity river transport to the oceans. *Glob. Biogeochem. Cycles* **17**.
- Atkinson T. C. (1977) Carbon dioxide in the atmosphere of the unsaturated zone: an important control of groundwater hardness in limestones. *J. Hydrol.* **35**, 111–123.
- Baldini J. U. L., Baldini L. M., McDermott F. and Clipson N. (2006) Carbon dioxide sources, sinks, and spatial variability in shallow temperature zone caves: evidence from Ballynamnra Cave, Ireland. *J. Caves Karst Stud.* **68**, 4–11.
- Balesdent J., Girardin C. and Mariotti A. (1993) Site-related  $\text{d}^{13}\text{C}$  of tree leaves and soil organic matter in a temperate forest. *Ecology* **74**, 1713–1721.
- Benavente J., Vadillo I., Carrasco F., Soler A., Liñán C. and Moral F. (2010) Air carbon dioxide contents in the vadose zone of a Mediterranean karst. *Vadose Zone J.* **9**, 126–136.
- Beverly, R.K., Beaumont, W., Tausz, D., Ormsby, K.M., von Reden, K.F., Santos, G.M., Southon, J.R., 2010. The Keck Carbon Cycle AMS Laboratory, University of California, Irvine: status report.
- Breecker D. and Sharp Z. D. (2008) A field and laboratory method for monitoring the concentration and stable isotope composition of soil  $\text{CO}_2$ . *Rapid Commun. Mass Spectrom.* **22**, 449–454.
- Breecker D. O., Payne A. E., Quade J., Banner J. L., Ball C. E., Meyer K. W. and Cowan B. D. (2012) The sources and sinks of  $\text{CO}_2$  in caves under mixed woodland and grassland vegetation. *Geochim. Cosmochim. Acta* **96**, 230–246.
- Breecker D. O., Bergel S., Nadel M., Tremblay M. M., Osuna-Orozco R., Larson T. E. and Sharp Z. D. (2015) Minor stable carbon isotope fractionation between respired carbon dioxide and bulk soil organic matter during laboratory incubation of topsoil. *Biogeochemistry* **123**, 83–98.
- Breecker D. O. (2017) Atmospheric  $p\text{CO}_2$  control on speleothem stable carbon isotope compositions. *Earth Planet. Sci. Lett.* **458**, 58–68.
- Center, C.D.I.A. Modern Records of Carbon and Oxygen Isotopes in Atmospheric Carbon Dioxide and Carbon-13 in Methane, Carbon Dioxide Information Analysis Center, Oak Ridge National Laboratory, U.S. Department of Energy. Path: [http://cdiac.ornl.gov/trends/co2/modern\\_isotopes.html](http://cdiac.ornl.gov/trends/co2/modern_isotopes.html).
- Cerling T. E. (1991) Carbon dioxide in the atmosphere: Evidence from cenozoic and mesozoic paleosols. *Am. J. Sci.* **291**, 377–400.
- Cerling T. E., Solomon D. K., Quade J. and Bowman J. R. (1991) On the isotopic composition of carbon in soil carbon dioxide. *Geochim. Cosmochim. Acta* **55**, 3403–3405.
- Clay G. and Worrall F. (2015a) Estimating the oxidative ratio of UK peats and agricultural soils. *Soil Use Manage.* **31**, 77–88.
- Clay G. D. and Worrall F. (2015b) Oxidative ratio (OR) of Southern African soils and vegetation: Updating the global OR estimate. *CATENA* **126**, 126–133.
- Cooke M. J., Stern L. A., Banner J. L. and Mack L. E. (2007) Evidence for the silicate source of relict soils on the Edwards Plateau, central Texas. *Quat. Res.* **67**, 275–285.
- Covington, M.D., 2015. The importance of advection for  $\text{CO}_2$  dynamics in the karst critical zone: An approach from dimensional analysis. *Geol. Soc. Spec. Pap.* 516, SPE516-509.
- Cowan B. D. (2010) *Temporal and spatial variability of cave-air  $\text{CO}_2$  in central Texas*. Department of Geological Sciences, The University of Texas, Austin.
- Cowan B. D., Osborne M. C. and Banner J. L. (2013) Temporal variability of cave-air  $\text{CO}_2$  in central Texas. *J. Caves Karst Stud.* **75**, 38–50.
- Data Tools: 1981 - 2010 Normals, Camp Mabry Station, Austin, TX. NOAA National Centers for Environmental Information. <http://www.ncdc.noaa.gov/cdo-web/datatools/normals>.
- Davidson E. A. and Trumbore S. E. (1995) Gas diffusivity and production of  $\text{CO}_2$  in deep soils of the eastern Amazon. *Tellus B* **47**, 550–565.
- Dilly O. (2001) Microbial respiratory quotient during basal metabolism and after glucose amendment in soils and litter. *Soil Biol. Biochem.* **33**, 117–127.
- Ek C. and Gewalt M. (1985) Carbon dioxide in cave atmospheres. New results in Belgium and comparison with some other countries. *Earth Surf. Proc. Land.* **10**, 173–187.
- Elliot W. R. and Veni G. (1994) *The caves and karst of Texas – 1994 NSS Convention Guidebook*. National Speleological Society, Huntsville, AL.
- Etheridge D. M., Steele L. P., Langenfelds R. L., Francey R. J., Barnola J.-M. and Morgan V. I. (1996) Natural and anthropogenic changes in atmospheric  $\text{CO}_2$  over the last 1000 years

- from air in Antarctic ice and firn. *J. Geophys. Res. Atmos.* **101**, 4115–4128.
- Faimon J., Licbinská M., Zajicek P. and Sracek O. (2012) Partial pressures of CO<sub>2</sub> in epikarstic zone deduced from hydrogeochemistry of permanent drips, the Moravian Karst, Czech Republic. *Acta Carsologica* **1**, 41.
- Fohlmeister J., Scholz D., Kromer B. and Mangini A. (2011) Modelling carbon isotopes of carbonates in cave drip water. *Geochim. Cosmochim. Acta* **75**, 5219–5228.
- Francey R. J., Allison C. E., Etheridge D. M., Trudinger C. M., Enting I. G., Leuenberger M., Langenfelds R. L., Michel E. and Steele L. P. (1999) A 1000 year high precision record of  $\delta^{13}\text{C}$  in atmospheric CO<sub>2</sub>. *Tellus B* **51**, 170–193.
- Frank D., Poulter B., Saurer M., Esper J., Huntingford C., Helle G., Treydte K., Zimmermann N., Schleser G. and Ahlström A. (2015) Water-use efficiency and transpiration across European forests during the Anthropocene. *Nat. Clim. Chang.* **5**, 579–583.
- Frisia S., Fairchild I. J., Fohlmeister J., Miorandi R., Spötl C. and Borsato A. (2011) Carbon mass-balance modelling and carbon isotope exchange processes in dynamic caves. *Geochim. Cosmochim. Acta* **75**, 380–400.
- Gao P., Xu X., Zhou L., Pack M. A., Griffin S., Santos G. M., Southon J. R. and Liu K. (2014) Rapid sample preparation of dissolved inorganic carbon in natural waters using a headspace-extraction approach for radiocarbon analysis by accelerator mass spectrometry. *Limno. Oceanogr. Methods* **12**, 174–190.
- Garcia-Anton E., Cuezva S., Fernandez-Cortes A., Benavente D. and Sanchez-Moral S. (2014) Main drivers of diffusive and advective processes of CO<sub>2</sub>-gas exchange between a shallow vadose zone and the atmosphere. *Int. J. Greenh. Gas Control* **21**, 113–129.
- Hendy C. H. (1971) The isotopic geochemistry of speleothems-I. The calculation of the effects of different modes of formation on the isotopic composition of speleothems and their applicability as paleoclimate indicators. *Geochim. Cosmochim. Acta* **35**, 801–824.
- Hesterberg R. and Siegenthaler U. (1991) Production and stable isotopic composition of CO<sub>2</sub> in a soil near Bern, Switzerland. *Tellus* **43B**, 197–205.
- Hockaday W. C., Masiello C. A., Randerson J. T., Smernik R. J., Baldock J. A., Chadwick O. A. and Harden J. W. (2009) Measurement of soil carbon oxidation state and oxidative ratio by <sup>13</sup>C nuclear magnetic resonance. *J. Geophys. Res.* **114**, G02014.
- Jackson R. B., Moore L. A., Hoffmann W. A., Pockman W. T. and Linder C. R. (1999) Ecosystem rooting depth determined with caves and DNA. *Proc. Natl. Acad. Sci. U. S. A.* **96**, 11387–11392.
- Keeling C. D. (1958) The concentration and isotopic abundances of atmospheric carbon dioxide in rural areas. *Geochim. Cosmochim. Acta* **13**, 322–334.
- Keeling, C.D., Whorf, T.P., 2005. Atmospheric CO<sub>2</sub> records from sites in the SIO air sampling network, Trends: A Compendium of Data on Global Change. Carbon Dioxide Information Analysis Center, Oak Ridge National Laboratory, U.S. Department of Energy, Oak Ridge, TN, pp. <http://cdiac.esd.ornl.gov/trends/co2/sio-keel-flask/sio-keel-flask.html>.
- Knierim K. J., Pollock E. D., Hays P. D. and Khojasteh J. (2015) Using stable isotopes of carbon to investigate the SEasonal variation of carbon transfer in a northwestern arkansas cave. *J. Caves Karst Stud.* **77**, 12–27.
- Massman W. J. (1998) A review of the molecular diffusivities of H<sub>2</sub>O, CO<sub>2</sub>, CH<sub>4</sub>, CO, O<sub>3</sub>, SO<sub>2</sub>, NH<sub>3</sub>, N<sub>2</sub>O, NO and NO<sub>2</sub> in air, O<sub>2</sub> and N<sub>2</sub> near STP. *Atmos. Environ.* **32**, 1111–1127.
- Mattey D., Atkinson T., Barker J., Fisher R., Latin J.-P., Durrell R. and Ainsworth M. (2016) Carbon dioxide, ground air and carbon cycling in Gibraltar karst. *Geochim. Cosmochim. Acta* **184**, 88–113.
- McDonough L., Iverach C., Beckmann S., Manefield M., Rau G., Baker A. and Kelly B. (2016) Spatial variability of cave-air carbon dioxide and methane concentrations and isotopic compositions in a semi-arid karst environment. *Environ. Earth Sci.* **75**, 1–20.
- Meyer K. W., Feng W., Breecker D. O., Banner J. L. and Guilfoyle A. (2014) Interpretation of speleothem calcite  $\delta^{13}\text{C}$  variations: Evidence from monitoring soil CO<sub>2</sub>, drip water, and modern speleothem calcite in central Texas. *Geochim. Cosmochim. Acta* **142**, 281–298.
- Natelhofer K. J. and Fry B. (1988) Controls on natural nitrogen-15 and carbon-13 abundances in forest soil organic matter. *Soil Sci. Soc. Am. J.* **52**, 1633–1640.
- Noronha A. L., Johnson K. R., Southon J. R., Hu C., Ruan J. and McCabe-Glynn S. (2015) Radiocarbon evidence for decomposition of aged organic matter in the vadose zone as the main source of speleothem carbon. *Quat. Sci. Rev.* **127**, 37–47.
- Oster J. L., Montañez I. P., Guilderson T. P., Sharp W. D. and Banner J. L. (2010) Modeling speleothem  $\delta^{13}\text{C}$  variability in a central Sierra Nevada cave using <sup>14</sup>C and <sup>87</sup>Sr/<sup>86</sup>Sr. *Geochim. Cosmochim. Acta* **74**, 5228–5242.
- Pape J. R., Banner J. L., Mack L. E., Musgrove M. and Guilfoyle A. (2010) Controls on oxygen isotope variability in precipitation and cave drip waters, central Texas, USA. *J. Hydrol.* **385**, 203–215.
- Peyraube N., Lastennet R. and Denis A. (2012) Geochemical evolution of groundwater in the unsaturated zone of a karstic massif, using the PCO<sub>2</sub> - SIC relationship. *J. Hydrol.* **430**, 13–24.
- Schubert B. A. and Jahren A. H. (2012) The effect of atmospheric CO<sub>2</sub> concentration on carbon isotope fractionation in C<sub>3</sub> land plants. *Geochim. Cosmochim. Acta* **96**, 29–43.
- Serrano-Ortiz P., Roland M., Sanchez-Moral S., Janssens I. A., Domingo F., Goddérís Y. and Kowalski A. S. (2010) Hidden, abiotic CO<sub>2</sub> flows and gaseous reservoirs in the terrestrial carbon cycle: Review and perspectives. *Agric. For. Meteorol.* **150**, 321–329.
- Smith A. C., Wynn P. M., Barker P. A. and Leng M. J. (2015) Drip water electrical conductivity as an indicator of cave ventilation at the event scale. *Sci. Total Environ.* **532**, 517–527.
- Southon J., Santos G., Druffel-Rodriguez K., Druffel E., Trumbore S., Xu X., Griffin S., Ali S. and Mazon M. (2004) The Keck carbon cycle AMS laboratory, University of California, Irvine: initial operation and a background surprise. *Radiocarbon*.
- Spötl C., Fairchild I. J. and Tooth A. F. (2005) Cave air control on drip water geochemistry, Obir Caves (Austria): Implications for speleothem deposition in dynamically ventilated caves. *Geochim. Cosmochim. Acta* **69**, 2451–2468.
- Stuiver M. and Polach H. A. (1977) Reporting of <sup>14</sup>C data. *Radiocarbon* **3**, 355–363.
- Whitaker F. F. and Smart P. L. (2007) Geochemistry of meteoric diagenesis in carbonate islands of the northern Bahamas: 1. Evidence from field studies. *Hydrol. Process.* **21**, 949–966.
- White W. B. (2013) Carbon fluxes in karst aquifers: sources, sinks, and the effect of storm flow/Tok ogljika v kraskih vodonosnikih: izvori, ponori in ucinki poplavnih tokov. *Acta Carsologica* **42**, 177.
- Wong C. and Banner J. L. (2010) Response of cave air CO<sub>2</sub> and drip water to brush clearing in central Texas: Implications for recharge and soil CO<sub>2</sub> dynamics. *J. Geophys. Res.* **115**, G04018.
- Wong C. I. and Breecker D. O. (2015) Advancements in the use of speleothems as climate archives. *Quat. Sci. Rev.* **127**, 1–18.
- Wood B. D., Keller C. K. and Johnstone D. L. (1993) In situ measurement of microbial activity and controls on microbial

- CO<sub>2</sub> production in the unsaturated zone. *Water Resour. Res.* **29**, 647–659.
- Wood W. W. and Petraitis M. J. (1984) Origin and distribution of carbon dioxide in the unsaturated zone of the southern high plains of Texas. *Water Resour. Res.* **20**, 1193–1208.
- Wynn J. G., Bird I. M. and Wong V. N. L. (2005) Rayleigh distillation and the depth profile of <sup>12</sup>C/<sup>13</sup>C ratios of soil organic carbon from soils of disparate texture in Iron Range National Park, Far North Queensland, Australia. *Geochim. Cosmochim. Acta* **69**, 1961–1973.
- Xu X., Trumbore S. E., Zheng S., Southon J. R., McDuffee K. E., Luttgen M. and Liu J. C. (2007) Modifying a sealed tube zinc reduction method for preparation of AMS graphite targets: reducing background and attaining high precision. *Nucl. Instrum. Methods Phys. Res. Section B: Beam Interactions with Mater. Atoms* **259**, 320–329.

*Associate Editor:* F. McDermott